E L E C T R O M A G N E T I C   I N T E R A C T I O N S

A rapporteur's summary given at the XIV International Conference
on High Energy Physics in Vienna

by

Samuel C.C. Ting

Department of Physics, and Laboratory for Nuclear Science,

Massachusetts Institute of Technology, Cambridge, Massachusetts /USA

and

Deutsches Elektronen-Synchrotron, DESY, Hamburg, Germany

E L E C T R O M A G N E T I C   I N T E R A C T I O N S

Samuel C.C. Ting

Department of Physics and Laboratory for Nuclear Science,
Massachusetts Institute of Technology, Cambridge, Mass./USA

and

Deutsches Elektronen-Synchrotron, DESY, Hamburg, Germany

!ty report to this conference consists of three closely related subjects:

Experiments to test quantum electrodynamics at small distances, leptonic decays of vector mesons, and photo-production of vector mesons.

As most of what I have to say is based on the validity of quantum electrodynamics at small distances, I will present my report in the order outlined above.

The important works on electron scattering, muon scattering, high precision quantum electrodynamics at small momentum transfers, photoproduction of bosons, etc. will be conveyed in Prof. Panofsky's and Prof. Richter's talk and will not be referred to here.

I. Quantum Electrodynamics at Small Distances:

A beautiful experiment from the Stanford - Princeton-colliding beam group was reported to this conference. [1]
In this experiment, two beams of electrons with 70mA current each at 550 MeV ∢ collided in an interaction region surrounded by a large solid angle counter-spark chamber system (Fig. 1).
Veto counters were used around the detector such that the cosmic-ray background was about 3%. Radiative corrections were kept small
(≃ 10%) by including events with radiated real photons up to more than 0.1E for radiation along the initial direction, and to ≃ 0.6E for radiation along the final direction.

The lowest order diagram for Møller scattering contains space-like virtual photons; this experiment can therefore be regarded as a test of space-like photon propagators and of the electron vertex function. The Møller cross section modified by the Feynman regulator and by a radiative correction is

$$\frac{d\sigma}{d\Omega}(\theta,K) = \frac{r_0^2}{8}\left(\frac{m}{E}\right)^2\left[\frac{s^4+q_0^4}{q^4}\,G_K^2(q^2) + \frac{2s^4}{q^2q_0^2}\,G_K(q^2)\,G_K(q_0^2)\right.$$

$$\left. + \frac{s^4+q^4}{q_0^4}\,G_K^2(q_0^2)\right]\left(1+\delta\right)$$

where

$$G_K(q^2) = \left(1-\frac{q^2}{K^2}\right)^{-1}, \quad s^2 = 4E^2, \quad q^2 = -4E^2\sin^2\theta/2, \quad q_0^2 = -4E^2\cos^2\theta/2$$

A value of zero for K^{-2} would be equivalent to $G_K(q^2) = 1$ consistent with a point-like electron and no cut-off on the photon-propagator.

The result, based on 7000 events, is $K^{-2} = -(.06 \pm .06)(GeV/c)^2$ which is consistent with $K^{-2} = 0$.

A series of large momentum transfer e^+e^- pair production experiments and wide angle bremsstrahlung experiments were also reported to this conference.

To first order three diagrams contribute to pair production (Fig. 2). The first two, the BH diagrams, can be calculated by Q.E.D. The last, the Compton diagram, cannot be calculated exactly, but experimental conditions can be chosen such that its contribution is small; in particular, since the e^+e^- pairs in the BH diagrams behave under charge conjugation as two photons (C = +1) and the BH cross section varies rapidly with angle ($\sim \theta^{-6}\dots\theta^{-8}$), whereas the Compton term behaves under C like one photon (C = -1) and the Compton cross section decreases smoothly with θ ($\sim \theta^{-3}$).
By choosing a symmetrical detector with small opening angles one eliminates the interference between the BH and Compton terms and at the same time suppresses the Compton term to a few percent level.

For symmetrical pairs with $\theta_- = \theta_+ \leq 10°$ the momentum transfer to the recoil nucleus $q \simeq E\theta^2 \leq 100$ MeV/c, while the mass of the virtual electron propagator t $\simeq \sqrt{2}E\theta \leq 1000$ MeV/c. Thus under these conditions a heavy nuclear target may be used with relatively small form factor corrections. The yield goes up as Z^2 and thus enables one to compare the measured e^+e^- rate with predictions of Quantum Electrodynamics to a momentum transfer of 1 GeV/c.

The DESY - M.I.T. group has reported a new result on pair production with a precision of $\pm$ 5% and up to a pair invariant mass of 1 GeV/c^2 [2]. This experiment, using the 7.5 GeV synchrotron and restricting the pair production angle to $\leq$ 7.7°, with carbon target, and with 4 high precision Čerenkov counters to reject pions, using fast electronics for handling accidentals, yields results, based on 400 - 1000 events at each point, which are in good agreement with the predictions of Quantum Electrodynamics. The result of their measurement, together with their first result on pair production with the same apparatus is shown in Fig. 2.

Following the analysis of Kroll, who shows, that correct application of the Ward identities of higher orders requires that modification of BH cross section must be of the form $\delta_{exp}/\delta_{BH} = 1 \pm (m/\Lambda)^n, n \geq 4$ where Λ is a cut-off parameter used as a standard of comparison between various experiments on Q.E.D., the DESY - M.I.T. group experiment yields a $\Lambda > 2$ GeV with 68% confidence level $(n = 4)$

Two beautiful experiments on wide angle bremsstrahlung were also reported. The diagrams of bremsstrahlung and pair production are identical if one interchanges $p_- \longrightarrow -p_-$ in figure 2. Thus the bremsstrahlung experiments enable one to probe time like virtual electron propagators whereas the pair production experiments test Q.E.D. with space-like virtual leptons.

The experiment by the Berkelman, Littauer group [3] used the internal beam of the Cornell 10 GeV electron synchrotron, carbon target, and counters to detect the scattered electron and photon in coincidence. Their set-up is shown in Fig. 3.

The scattered electrons were detected at 6.4° by a single focusing spectrometer, and the photon aperture was defined by a collimator at 6.2°. The photons were detected by lead glass counters. Time of flight and pulse height information were used to select the $e-\gamma$ events from background. 100 events were collected at each point and their result as a function of final state mass M is shown in Fig. 3. The best straight line fit to these points is $R = 0.94 \pm 0.14 + (0.9 \pm 1.9) \times 10^{-4}$ M; the results are consistent with Q.E.D. which predicts a straight line at 1.0 with zero slope.

The experiment of Bernardini's group [4] at Frascati used a hydrogen target and counter techniques to detect the final proton, electron, and γ in triple coincidence up to a (e, γ) invariant mass of 100 MeV/c^2. Their results also agree with Q.E.D.

The summary of the three latest experiments on Q.E.D. is shown in Figure 4, which clearly gives us confidence that first order quantum electrodynamics of electrons and photons is valid, to at least 5% level, in both the space-like and time-like region, and up to a momentum transfer of 1 GeV/c with a corresponding cut-off $\Lambda \sim 2$ GeV at a 68% confidence level.

II. Leptonic Decays of Vector Mesons

Having obtained some experimental evidence on the validity of quantum electrodynamics at momentum transfers up to 1 BeV/c, we turn to experiments on the detailed understanding of the nature of light.

The rest of the talk will be on experiments designed to measure the coupling between photons and vector mesons (massive photons, which have the same quantum numbers as the photon $J = 1$, $C = -1$, $P = -1$, but with non-zero rest mass) and the photoproduction of vector mesons.

MOTIVATION

The purposes of studying leptonic decays of vector mesons are fourfold (A, B, C, D): [5]

A. Measuring the branching ratio $BR = \dfrac{V^{\circ} \rightarrow \ell^{+} + \ell^{-}}{V^{\circ} \rightarrow \text{all modes}}$

is the only direct way to determine the coupling constant between the vector mesons ρ, ω, ϕ and the γ ray.

The coupling constant γ_V is related to the partial decay width $\Gamma(V^{\circ} \rightarrow \ell^{+} + \ell^{-})$ via:

$$\frac{\gamma_V^2}{4\pi} = \frac{\alpha^2}{12} \frac{m_V}{BR \cdot \Gamma_{tot}} = \frac{\alpha^2}{12} \cdot \frac{m_V}{\Gamma(V^{\circ} \rightarrow \ell^{+} + \ell^{-})} \qquad (2)$$

The precise knowledge of γ_V or $\Gamma(V^{\circ} \rightarrow \ell^+ \ell^-)$ enables us to determine the $\omega - \phi$ mixing angles directly via

$$\tan \theta = \frac{m_\omega}{m_\phi} \tan \theta_\gamma = \frac{m_\phi}{m_\omega} \tan \theta_B$$

$$\frac{\Gamma(\omega \rightarrow \ell^+ \ell^-)}{\Gamma(\phi \rightarrow \ell^+ \ell^-)} = \frac{m_\omega}{m_\phi} \tan^2 \theta_\gamma = \frac{m_\phi}{m_\omega} \tan^2 \theta = \frac{\gamma_\phi^2}{\gamma_\omega^2} \qquad (3)$$

to check Weinberg's first sum rule which is based on the current mix-ing model and predicts

$$\frac{1}{3} \frac{m_\rho^2}{\gamma_\rho^2} = \frac{m_\omega^2}{\gamma_\omega^2} + \frac{m_\phi^2}{\gamma_\phi^2} \qquad (4)$$

To compare it with quark model calculations of Dar and Weisskopf: [6]

$$\Gamma(\rho \rightarrow ee) = 5.8 \text{ keV}, \quad \Gamma(\phi \rightarrow ee) = 0.95 \text{ keV} \qquad \text{etc.}$$

In particular, the quantity γ_V appears directly in the vector dominance model approximation, which relates the electromagnetic current $J_\mu(x)$ of the hadrons to the phenomenological fields

$$\rho_\mu(x), \ \omega_\mu(x), \ \phi_\mu(x) \qquad \text{of the vector mesons via:}$$

$$J_\mu(x) = -\left[\frac{m_\rho^2}{2\gamma_\rho} \rho_\mu(x) + \frac{m_\omega^2}{2\gamma_\omega} \omega_\mu(x) + \frac{m_\phi^2}{2\gamma_\phi} \phi_\mu(x) \right] \qquad (5)$$
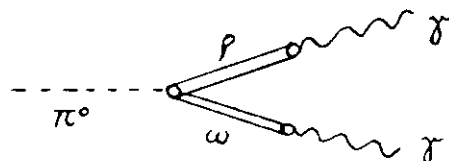
Thus in the vector dominance model, the knowledge of γ_V is essential to our understanding of the electromagnetic form factors of nucleons and of pseudoscalar mesons, and to our understanding of the electro-magnetic decays of mesons.

For example,[7] the simple vector dominance model calculates the pion form factor from the graph
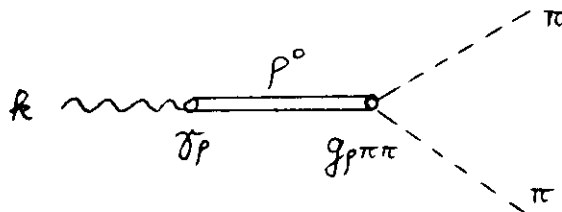
giving the result $F(k^2) = \dfrac{g_{\rho\pi\pi}}{2\gamma_\rho} \cdot \dfrac{m_\rho^2}{m_\rho^2 - k^2}$ $\qquad (6)$

where $g_{\rho\pi\pi}$ can be calculated from the width of $\rho \rightarrow \pi\pi$ and the normalization condition $F_\pi(o) = 1$ gives $g_{\rho\pi\pi} = 2\gamma_\rho$ and the decay of $\pi^\circ \rightarrow 2\gamma$ according to

which gives

$$\Gamma(\pi^\circ \to 2\gamma) = \frac{\alpha^2}{192} \left(\frac{\gamma_\rho^2}{4\pi}\right)^{-1} \left(\frac{\gamma_\omega^2}{4\pi}\right)^{-1} \frac{f_{\rho\pi\omega}^2}{4\pi} \frac{m_\pi^3}{3} \qquad (7)$$

Thus $\qquad \dfrac{\Gamma(\omega \to \pi^\circ + \gamma)}{\Gamma(\pi^\circ \to 2\gamma)} \qquad$ depends only on $\dfrac{\gamma_\omega^2}{4\pi}$.

B. Comparing the rates of $V^\circ \to e^+ + e^-$ vs. $V^\circ \to \mu^+ + \mu^-$ gives us a direct check of μ, e universality in the time-like region and at the high momentum transfers of $q^2 = M_V^2 > 0$. This probes any possible differences in the form factors F_e (q^2) and F_μ (q^2) between electrons and muons in a domain which cannot be covered by either elastic scattering experiments ($\mu + p \to \mu + p$ vs. $e + p \to e + p$ with $q^2 < 0$) or low momentum transfer experiments like the $(\frac{g-2}{2})$ e vs. $(\frac{g-2}{2})\mu$.

C. In principle, studying the $e^+ e^-$ mass spectrum from reactions like $\gamma + C \to C + V^\circ \to \ell^+ + \ell^-$ and $e^+ e^- \to \pi^+ \pi^-$ or $e^+ e^- \to K^+ K^-$ gives us the best way to determine the mass M_V and the width Γ_V of the vector mesons. This is because the background contribution to the mass peak $V^\circ \to \ell^+ + \ell^-$ can be calculated exactly.

D. It follows from (5) that the photo-production cross section of vector mesons can be related to the vector meson nucleon cross sections directly via [8]

$$\sigma(\gamma + A \to B + C) = \sum_V \frac{\alpha \pi}{\gamma_V^2} \sigma_{tot} (V + A \to B + C) \qquad (8)$$

This part of the physics I will discuss in detail later on.

EXPERIMENTAL CONSIDERATIONS

There are two ways to study the leptonic decays of vector mesons: (A) From measuring the relative rates of production of vector mesons (via strong interactions) and the rate of vector meson decay into $\ell^+\ell^-$ pairs. And (B) from measuring the rates of vector meson decays in storage rings.

For both cases the best way to measure the branching ratio $BR = V \rightarrow \ell^+\ell^- / V \rightarrow$ all is to detect all final state decay particles $V_o \longrightarrow x + y \ldots$ with a 4π detector. In such a case the branching ratio follows directly without any phase-space and acceptance corrections. In practice, however, since one can only detect the final state particles within a rather limited solid angle, the angular distribution of all final state particles must be measured in order that the yields of $V_o \longrightarrow \ell^+\ell^-$ pairs and $V_o \longrightarrow$ all modes be corrected for different acceptances.

(A) For Production Experiments:

It follows from a general analysis by Oakes [9], based on invariance arguments, that the $\ell^+\ell^-$ pair production from any unpolarized initial state of strongly-interacting particles is completely described by five real form factors, that are simply related to the density-matrix elements for the production of a virtual photon, which then decays into the pair. By measuring the angular distribution and polarization of the pair, one can determine all five form factors (or their density-matrix equivalents) and thereby also investigate the structure of the production process.

In the center of mass of the $\ell^+\ell^-$ pair, (taking the incident beam direction along the z-axis and the normal to the production plane along the y-axis)
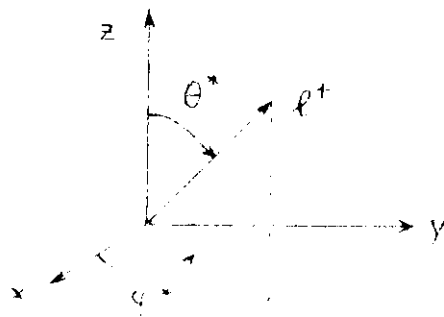
the angular distribution of the decay of a vector meson into two
spinless particles $x^+ x^-$ is :

$$W_{x^+ x^-}(\theta^*, \varphi^*) = N^1 (\rho^{11} \sin 2\theta^* + \rho^{00} \cos^2 \theta^*$$
$$- \rho^{1-1} x \sin^2 \theta^* \cos 2\varphi^* - \sqrt{2} \, \text{Re} \, \rho^{10}$$
$$x \sin 2\theta^* \cos \varphi^*) \ldots\ldots\ldots \quad (9)$$

and the angular distribution of the $V^0 \longrightarrow \ell^+ \ell^-$ is

$$W(\theta^*, \varphi^*) = (1 - \frac{W_{x^+ x^-}}{N^1}(\theta^*, \varphi^*))/ \frac{8\pi}{3} \quad \ldots\ldots \quad (10)$$

The following cases of (9) and (10) are of special interest:

1. If V^0 mesons are produced by an incident beam of high-
energy π mesons, in the one-meson-exchange approximation either G-
even or G-odd states can be exchanged. For the G-odd exchange -- the
case of ρ^0 production via one-pion-exchange mechanism -- we have
$\rho^{00} = 1$ and $\rho^{i,j} = 0$, where i or j $\neq 0$.

Thus we have:

$$W(\rho \rightarrow \pi^+ \pi^-)(\theta^*, \varphi^*) = \frac{3}{4\pi} \cos^2 \theta^* \text{ (independent}$$
of φ^*)
$$\ldots\ldots\ldots \quad (11)$$

$$W(\rho \rightarrow \ell^+ \ell^-)(\theta^*, \varphi^*) = \sin^2 \theta^* \times \frac{3}{8\pi} \ldots\ldots\ldots \quad (12)$$

For the G-even exchange -- the case of ω^0 production via ρ^0
exchange -- we have $\rho^{11} = \bar{\rho}^{-1-1}$, $\rho^{1-1} \neq 0$, all other $\rho^{i,j} = 0$.
Thus for $\omega \longrightarrow \ell^+ \ell^-$ we have:

$$W(\omega \rightarrow \ell^+ \ell^-)(\theta^*, \varphi^*) = \frac{1 - \frac{1}{2}\sin^2 \theta^*(1 - 2\rho^{1-1} \cos 2\varphi^*)}{8\pi/3} \text{ (depends on } \varphi^*\text{)}$$
$$\ldots\ldots\ldots\ldots\ldots\ldots \quad (13)$$

and on averaging over the azimuthal angle φ^* one obtains

$$W(\omega \rightarrow \ell^+ \ell^-)(\theta^*, \varphi^*) = \frac{3}{16\pi}(1 + \cos^2 \theta^*) \quad \ldots\ldots\ldots \quad (14).$$

Thus measuring the decay angular spectrum of $\rho \rightarrow \ell^+ \ell^-$ (the θ, φ
dependence) and the value of the density matrix, as a function of moment-
um transfer, yields us information on the production mechanism of ρ^0, as
well as determining the $\omega \longrightarrow \ell^+ \ell^-$ contamination in the $\rho^0 \rightarrow \ell^+ \ell^-$
spectrum.

2. For a beam of high energy photons incident on complex nuclei, coherent production of ϕ in the forward region requires that ϕ and the incident photon carry the same spin orientation, and thus we have

$$W_{\phi \to KK}(\theta^*, \varphi^*) = \frac{3}{8\pi} \sin^2 \theta^* \quad \dots\dots\dots\dots\dots \quad (15)$$
$$\text{(P wave decay)}$$

and

$$W_{\phi \to \ell\ell}(\theta^*, \varphi^*) = \frac{3}{16\pi}(1 + \cos^2 \theta^*) \quad \dots\dots\dots\dots \quad (16)$$
$$\text{(S and D wave decay)}$$

(B) For Colliding Beam Experiments:

The annihilation of $e^+ e^-$ into n spinless bosons through the one - photon channel leads [10] to a final state with $P = -1$, $C = -1$, $J = 1$, $T = 1$ for n even, $T = 0$ for n odd. If $\vec{J}$ is the most general vector (pseudo vector for n odd) formed out of independent final momenta for even (odd) number of bosons the final distribution can be shown to have the general form

$$\frac{1}{2}|\vec{J}|^2 \sin^2 \theta \tag{17}$$

where θ is the angle formed between $\vec{J}$ and the initial line of collision. Thus for

$$e^+ + e^- \longrightarrow \rho \longrightarrow \pi_1^+ \pi_2^-$$
$$\longrightarrow \phi \longrightarrow K_1^+ K_2^-$$
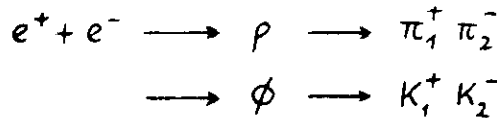
the only vector is $\vec{P_1} - \vec{P_2}$ and we get a $\sin^2 \theta^*$ distribution.

For $e^+ e^- \longrightarrow \omega \longrightarrow 3\pi$ the only pseudo vector is the normal to the production plane, and we have the normal with a $\sin^2 \theta$ - distribution around the initial line of collision.

Assuming a Breit-Wigner description for the resonance cross-section near its maximum, we have then

$$\sigma(E^2) \simeq \frac{2J+1}{4} \frac{\Gamma_i \Gamma_f}{(2E-m)^2 + \Gamma^2/4} \quad , \text{ where } \Gamma_i, \Gamma_f$$

are the rates into initial $e^+ e^-$ and final state, respectively.

If the energy resolution in C.M. is $2\Delta E$ and if $\Gamma \gg 2\Delta E$

we then have
$$\overline{\sigma}_R = \frac{1}{\Delta E} \int_{\frac{1}{2}(m - \Delta E)}^{\frac{1}{2}(m + \Delta E)} \sigma(E)\, dE$$

or

$$\sigma_R = \sigma(2m) = \pi \lambda^2 (2J + 1)\, B_i\, B_f$$

where B_i, B_f are the branching ratios for decay into initial and final state, respectively. For our case $J = 1$, $\lambda = \dfrac{2}{m}$

$$\sigma_R(\text{Breit-Wigner}) = \frac{12\pi}{m_\rho^2} \cdot \frac{\Gamma_{ee}}{\Gamma_\rho} \tag{18}$$

Thus the cross section [18] at the peak determines the branching ratio of leptonic decays of vector mesons.

For case of $\rho \rightarrow \pi^+\pi^-$ and $\phi \rightarrow K^+K^-$ pairs the differential cross section in the c.m. system is

$$\frac{d\sigma}{d\Omega}(\theta) = \frac{\pi \alpha^2}{16} \cdot \frac{1}{E^2} \left| F(K^2) \right|^2 \sin^2 \theta \tag{19}$$

where $F(K^2)$ is the e.m. form factor of π or K .
Thus measuring this cross section also enables one to determine the e.m. form factors of π and K mesons in the time like region.

The cross section as a function of energy:

$$\sigma = C \frac{m_\rho^4}{(4E^2 - m_\rho^2)^2 + m_\rho^2 \Gamma_\rho^2} \tag{20}$$ allows us to

make a unique determination of mass and width of the vector mesons.

EXPERIMENTAL RESULTS:

The Branching Ratio of $\rho \longrightarrow \ell^+\ell^-$:

Many experiments have been done on the branching ratio of $\rho \longrightarrow \ell^+\ell^-$,
such as the experiment done by the North-Eastern -M.I.T. group at
C.E.A. [11] etc. All these experiments yield results consistent with
each other. But the resolutions of these experiments are not pre-
cise enough to make a definite statement on the width of ρ°.

The results of the DESY - M.I.T. group [12] on the $\rho \longrightarrow e^+e^-$ is
shown in Fig. 5. This experiment is done with a precision spectro-
meter with a mass resolution of $\pm$ 15 MeV/c^2. To reduce systematic
errors, both the production of ρ° and the subsequent $\rho^\circ \longrightarrow e^+e^-$
decay were measured with the same apparatus . The experiment was
done at a low photon energy of 2.7 GeV on a carbon (T=0) target,
such that the $\omega \longrightarrow e^+e^-$ contamination is small.
At low energy, the bubble chamber data show that photoproduction of
ω on protons is consistent with O.P.E. No ω contamination
was observed and the measured $\rho \longrightarrow e^+e^-$ width is 120 $\pm$ 20 MeV/c^2.
The branching ratio is obtained by dividing the area under the two
curves and it yields

$$BR = (6.4 \pm 1.5) \times 10^{-5}.$$

The result of the beautiful experiment done by Wilson's group [13]
at the A.G.S. is also shown in the same figure. This experiment
yields a BR = $(5.8 \pm 1.2) \times 10^{-5}$ and a width of 97 $\pm$ 20 MeV.

Two beautiful experiments on the branching ratio and width of the ρ^{o} were done by the Novosibirsk[14] and the Orsay[15] colliding beam groups. Fig. 6 shows some of the importatnt characteristics of the storage rings used by these groups together with the ring used to test QED by the Stanford group.

Both groups measured the $e^{+}e^{-}$ - annihilation into $\pi^{+}\pi^{-}$. The two experimental set-ups are very similar. Fig. 7 shows the Orsay one. They used thin plate spark chambers to measure the angles of the particles, range and shower spark chambers to distinguish pions from electrons and muons, coincidence counter arrangements triggered in phase with the beam bunches and additional veto counters to reduce cosmic ray background.

The result of the $e^{+}+e^{-} \longrightarrow \rho \longrightarrow \pi^{+}+\pi^{-}$ spectrum from Orsay is also shown in Fig. 7 and the following table summarizes the results of the two colliding beam experiments together with earlier results from DESY-M.I.T. and from Harvard groups.

	m_ρ (MeV)	Γ_ρ (MeV)	BR $\times 10^{5}$	$\Gamma_{\rho \to ee}$ (keV)
Novosibirsk	754 ± 9	105 ± 20	5.0 ± 1.0	
Harvard		97 ± 20	5.8 ± 1.2	
Orsay	760 ± 4	112 ± 12	6.54 ± 0.72	7.13 ± 0.51 (from their fit)
DESY / M.I.T.			6.4 ± 1.5	
Average	759 ± 4.0	108 ± 8.5	6.04 ± 0.50	6.52 ± 0.75 (from average BR)

$$\frac{\gamma_\rho^{2}}{4\pi} = \frac{\alpha^{2}}{12} \frac{m_\rho}{\Gamma_{\rho \to ee}} = 0.52 \begin{array}{c} +0.07 \\ -0.06 \end{array}$$

for the coupling constant when the ρ-meson is on the mass shell.

Using $\dfrac{\gamma_\rho^{2}}{4\pi} = \dfrac{3\Gamma_o}{m_o} \left(1 - \dfrac{4 m_\pi^{2}}{m_o^{2}}\right)^{-3/2}$ from π form factor we have:

$\dfrac{\gamma_\rho^{2}}{4\pi} = 0.53 \pm 0.04$ for the coupling constant when the photon is on the mass shell.

(2) The Branching Ratio of $\phi \longrightarrow \ell^+ \ell^-$

An experiment was performed at DESY by the DESY - M.I.T. group, using a precision spectrometer and counter techniques. The experiment is very similar to the experiment this group has done on the ρ^o meson and it has the following major experimental facts:

1. Normalization and polarization:

They have measured both the production of ϕ by photons on carbon (with 10^4 events) and the decay of $\phi \longrightarrow e^+ e^-$ (with 40 events), with the same apparatus, thus reducing the major systematic errors in the normalization. Their system has a mass resolution of $\pm$ 5 MeV/c^2 for $\phi \longrightarrow K^+ K^-$ events, and of $\pm$ 20 MeV/c^2 for $\phi \longrightarrow e^+ e^-$ events. With 10^4 events they find that photoproduction of ϕ on complex nuclei is via diffraction mechanism. Thus the angular distribution for K-pairs is $W_{KK} = \frac{3}{8\pi} \sin^2 \theta^*$, for electron pairs

$$W_{ee} = \frac{3}{16\pi}\left(1 + \cos^2\theta^*\right)$$

2. QED pair contamination in the yield:

To first order both the Bethe-Heitler and ($\phi \rightarrow e^+ e^-$) diagrams contribute to the reaction

$$\gamma + C \longrightarrow C + e^+ + e^-$$
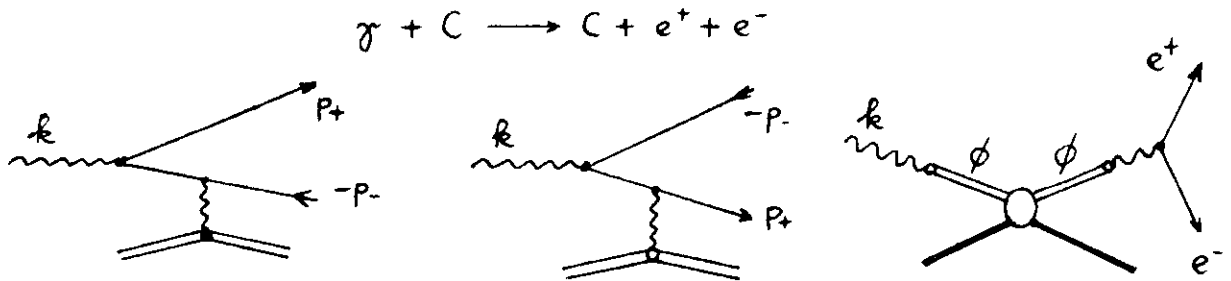
However, since the BH cross section varies rapidly with angle ($\sim \theta^{-6}$), while the $\phi \longrightarrow e^+ e^-$ cross section varies slowly with angle, the signal ($\phi \longrightarrow e^+ e^-$)/background (BH - $e^+ e^-$-pairs) $\sim \theta^3$.

To reduce BH background the $e^+ e^-$ -pair was measured at large angles of 22° - 30°. The BH background under the narrow ϕ peak is then $< \frac{1}{2}$ of the total yield.

3. Since the ρ^o has a large width, the $\rho \rightarrow e^+e^-$ yield contaminates the $\phi \rightarrow$ ee spectrum. However, since the ϕ has a narrow width, a good mass resolution on e^+e^- will enable one to pick out the peak with a small ρ background. Using the $\rho \rightarrow e^+e^-$ spectrum measured in the same apparatus and with the measured diffraction (pure imaginary amplitude) cross section, they estimate an overall 10% contamination of ρ plus (ρ, ϕ) interference under the ϕ peak.

Figure 8 shows the resulting $\phi \rightarrow K^+K^-$ and $\phi \rightarrow e^+e^-$ spectrum. Integrating the area under the spectra one obtains directly

$$\Gamma(\phi \rightarrow e^+e^-)/\Gamma(\phi \rightarrow K^+K^-) \quad = (5.7 \pm 1.7) \times 10^{-4}.$$

Using $\Gamma(\phi \rightarrow K^+K^-)/\Gamma(\phi \rightarrow all) = 0.473$ one gets
BR = $(2.70 \pm 0.80) \times 10^{-4}$.

A beautiful but difficult experiment on the ϕ branching ratio was reported by the Orsay Colliding Beam Group.[17] Since they have both electrons and positrons in one ring two beams of equal energy of 510 MeV/c^2 collided   and produced ϕ's at rest, since each K meson has a mass of $\simeq$ 500 MeV/c^2, there is very little Q-value in the ϕ decay and the charged K-pairs do not escape the wall of the vacuum chamber to be detected. This experiment is done by detecting the $\pi^+\pi^-$ pairs from the $\phi \rightarrow K_L^o K_S^o$
$$\hookrightarrow 2\pi$$
decay and by detecting the $\pi^+\pi^-\pi^o$'s from ϕ decay directly.

(Since ϕ is a vector meson (in pure C = -1 state) it does not decay into K_1K_1 or K_2K_2 pairs. It only has the $\phi \rightarrow K_1K_2$ mode.)

$\underline{K_1K_2 \text{ decay}}$: The K_1K_2 decays were identified by the two charged π's of the charged decay mode of the K_1. The angle θ between the 2 π-mesons is close to 180° and always larger than a minimum angle given by kinematics (θ = 150° at 2E = m_ϕ). This was a very efficient criterion for the identification of the K_1 decays. The range of the π's is rather short and provides another criterion. The result of this part of the experiment (based on 150 events , and using the branching ratio $B(\phi \rightarrow K_1K_2) = 0.389 \pm 0.031$) yields a BR = $(3.10 \pm 0.5) \times 10^{-4}$.

This is in good agreement with the earlier DESY - M.I.T. results of

$(2.7 \pm 0.8) \times 10^{-4}$.

$\pi^+ \pi^- \pi^°$ - decay: Again two charged π's were detected. The corresponding angle θ is not peaked close to $180°$ and the range of these π's is usually larger than in the $K_S^°$ case. Here, the kinematics cannot be reconstituted. The efficiency of the detection system for 3 π-decays is weaker and has been computed by Monte Carlo method to be 4%. This, combined with the smaller branching ratio of the ϕ for 3 π-decay, leads to roughly three times less ϕ's, being detected through this mode. Using the value $B(\phi \rightarrow 3\pi) =$ 0.138 ± 0.043 this part of the measurement yields a BR = $(5.8 \pm 1.4) \times 10^{-4}$. This is in strong disagreement with the more precise result above. TheOrsay group has also measured the various branching ratios for ϕ decay and they find the values:

$$B(\phi \rightarrow K^+ K^-) / B(\phi \rightarrow K_1 K_2) / B(\phi \rightarrow 3\pi) = 0.48 \pm 0.024 \ / \ 0.312 \pm 0.016 \ / \ 0.208 \pm 0.04$$

This is some-what different from the results obtained from the Rosenfeld Table:

$$B(K^+ K^-) \ / \ B(K_1 K_2) \ / \ B(3\pi) \quad = 0.473 \pm 0.032/0.389 \pm 0.031/0.138 \pm 0.043.$$

From this they obtain, using the $K_S^°$ events:

$$BR(\phi \rightarrow e^+ e^-) = (3.9 \pm 0.62) \times 10^{-4}; \quad \Gamma_{\phi \rightarrow ee} = (1.62 \pm 0.26) \text{ KeV}.$$

It is worthwhile to point out that both the DESY-M.I.T. group experiment and the Orsay storage ring experiment are very difficult experiments. In the DESY experiment the counting rate is almost one count / day. Thus it was entirely possible to run 3 days without any counts. 100 events represent a major effort to keep the detection system from changing. The Orsay experiment has the difficulties outlined already. Thus it is very gratifying to see that these two very different experiments yield the same result.

The first successful experiment on ϕ and ω decay and thus determining directly the mixing angle was done at CERN by the Zichichi-group (Fig. 9) with a [18] 1.93 GeV/c π^- beam. They studied the decay $\phi \rightarrow e^+ e^-$ via the reaction $\pi^- p \rightarrow$ $n V^°_{\rightarrow} e^+ e^-$. The mass of $V^°$ was determined to ± 15 MeV by measuring the velocity and direction of the neutron. In addition, the decay of $V^° \rightarrow e^+ e^-$ was measured by the opening angle and the energy of the electron pairs. A total

of 9 ± 3 events was observed. Normalize this yield to the production cross section from bubble chamber data they obtain a branching ratio BR = (6.1 ± 2.6) x 10^{-4} and a corresponding $\Gamma(\phi \rightarrow e^+e^-)$ = 2.1 ± 0.9 keV (using Γ_{tot} = 3.4 ± 0.8 KeV).

The following table summarizes the results of measurements on $\phi \rightarrow \ell^+\ell^-$. Together with the new results from Orsay of Γ_{tot} = 4.2 ± 0.9 these results yield, for the first time, an accurate value of $\gamma_\phi^2/4\pi$:

Groups	Γ_ϕ (MeV)	BR x 10^4	$\Gamma_{\phi \rightarrow ee}$ (keV)
DESY / M.I.T.		2.7+0.8	
Orsay	4.2+0.9	3.9+0.62	1.62±0.26 (from their best fit)
CERN		6.1±2.6	
Average	4.2±0.9	3.55±0.48	

From these we have: $\Gamma(\phi \rightarrow e^+e^-)$ = 1.49 ± 0.35 keV.

$$\gamma_\phi^2/4\pi = 3.04 \begin{smallmatrix}+1.07\\-0.66\end{smallmatrix}$$

(3)   The Branching Ratio of $\omega \rightarrow \ell^+\ell^-$:

An experiment was done at CERN by the Zichichi group[18] with the same techniques they have used on ϕ (Fig. 9). Taking the ρ-ω interference to be zero and using the known production angular distributions they obtained a branching ratio of BR = (0.40 ± 0.15) x 10^{-4} or $\Gamma_{\omega \rightarrow ee}$ = 0.49 ± 0.19 KeV.

The Orsay group of Lehmann, Marin, Lefrancois[19] has just finished a beautiful experiment on $e^+ + e^- \rightarrow \omega \rightarrow \pi^+\pi^-\pi^0$ by detecting the $\pi^+\pi^-$. The three body events were identified and separated from two body events and background by selecting events giving two non-collinear tracks originating from the beam. The resulting spectrum, obtained with the same apparatus as the ρ and ϕ experiments, is shown in Fig. 10. This experiment yields a branching ratio = (0.85 ± 0.16) x 10^{-4}, and a best fit $\Gamma_{\omega \rightarrow e^+e^-}$ = 1.04 ± 0.19 KeV.

From the average of these two branching ratios, we obtain a $(BR)_{av}=$ $(0.61 \pm 0.11) \times 10^{-4}$. This together with the world data on the width of ω (both groups prefer this value) of 12.2 ± 1.3 MeV, we obtain:

$$(\Gamma_{\omega \to e^+ e^-})_{av} = 0.744 \pm 0.156 \text{ KeV.}$$

$$(\gamma_\omega^2 / 4\pi)_{av} = 4.69 \begin{array}{c} +1.24 \\ -0.81 \end{array}$$

The Dubna group of Baldin[20] has also observed the $e^+ e^-$ decay mode of ρ, ω and ϕ . The experiment was done by measuring the reaction

$$\pi^- + p \longrightarrow V^0 + n \to e^+ + e^- + n$$

The conditions of the experiment allowed to detect, with high constant efficiency, the $e^+ e^-$ pairs in the mass range from 500 to 1200 MeV. (Fig.11). For each event, their system makes it possible to measure three parameters, the energies E_1 and E_2 of electrons from V^0 decay. And the opening angle θ between them. The knowledge of the above three parameters allows to calculate the effective mass of the event. Assuming a mixing angle of 38° (which, as we shall see, is a valid assumption, consistent with existing data), this experiment yields $B_\rho = (5.3 \pm 1.1) \times 10^{-5}$,

$B_\omega = (6.5 \pm 1.3) \times 10^{-5}$ and $B_\phi = (6.6 \begin{array}{c} +4.4 \\ -2.8 \end{array}) \times 10^{-4}$.

The work of Binnie et al[21] from the Rutherford Laboratory used the reaction $\pi^- + p \to \phi + n$, at 1.58 GeV/c to study both the production and the leptonic decay rates of ϕ . The $K^+ K^-$ mode was selected by scintillation counters and threshold water Čerenkov counter and spark chambers. The $e^- e^+$ decay of the was selected via thin foil optical spark chambers, lead plates, and scintillation counters. This experiment yields a result of BR = $(7.2 \pm 3.9) \times 10^{-4}$ or $\Gamma_{\phi \to e^+ e^-} = 2.4 \pm 1.5$ KeV or

$$(\gamma_\phi^2 / 4\pi) = 1.9 \begin{array}{c} +2.9 \\ -0.7 \end{array}.$$

Binnie et, al, also measured the Branching Ratio of $\omega \to e^+ e^-$, based on 3 events. They give a ratio lying between 5×10^{-5} and 6×10^{-4}.

These results are in agreement with other measurements before.

In Summary:

The large amount of accurate data on leptonic decays of vector mesons (ρ, ω, ϕ) from both production experiments and colliding beam experiments are in good agreement with each other. The average results of the three independent experiments plotted on the Sakurai circule (based on Weinberg's first sum rule) are shown in Fig. 12. These results yield the values of generalized mixing angle θ of:

CERN $\qquad \theta = 23° \begin{smallmatrix} +7° \\ -5° \end{smallmatrix}$

ORSAY $\qquad \theta = 35.1° \pm 3.3°$

DESY-M.I.T. $\qquad \theta = 40° \begin{smallmatrix} +5° \\ -7° \end{smallmatrix}$ (using $\Gamma_{\omega \to ee} = 1.04 + 0.19$ keV from Orsay).

Average $\qquad \theta = 31.6° \begin{smallmatrix} +3.9° \\ -4.9° \end{smallmatrix}$

The average value of θ is obtained from the average values of BR above.

The comparison of the average values of $V° \to \ell^+ \ell^-$ with various theoretical models is shown in the Table:

Decay	Average Experimental Results						Theoretical Models				
	BR	Γ_{tot} (MeV)	$\Gamma_{V \to \ell\ell}$ (keV)	$\frac{\gamma_V^2}{4\pi}$	γ_V^{-2}	Group	SU_3	Sakur.	DMO	Quark D.W.	Mass mix. K.L.Z.
$\rho \to e^+ e^-$	$6.04 \pm .50 \times 10^{-5}$	108.0 ± 8.5	$6.52 \pm .75$	$+.07 \\ 0.52 \\ -.06$	9	DESY-MIT NOVOSIB. ORSAY HARV.	9	9	9	$\Gamma_{V \to ee}$ 5.7 keV	$\Gamma_{V \to ee}$ keV
$\phi \to e^+ e^-$	$3.55 \pm .48 \times 10^{-4}$	$4.2 \pm .9$	$1.49 \pm .35$	$+1.07 \\ 3.04 \\ -.66$	$+.43 \\ 1.54 \\ -.40$	CERN DESY-MIT ORSAY	2	1.33	1.34	0.95	1.2
$\omega \to e^+ e^-$	$6.1 \pm 1.1 \times 10^{-4}$	12.2 ± 1.3	$0.74 \pm .16$	$+1.24 \\ 4.69 \\ -.81$	$+.21 \\ 1.00 \\ -.21$	CERN ORSAY	1	0.65	1.21	0.61	0.6

In conclusion:

(1) The data agree with the prediction of Weinberg's first sum rule - based on the current mixing model. It should be noted, however, that the Orsay result, without any finite width correction on Γ_ρ , are 1.8 standard deviations away from the predictions of Weinberg's first sum rule.

(2) The average values of the partial widths of $V^o \longrightarrow e^+ e^-$ agree remarkably well with the quark model calculations of Dar and Weisskopf.

(3) Both the Orsay data and the DESY/M.I.T. data prefer the mixing angle $\theta = 39^\circ$ given by Das, Mathur, Okubo [22], whereas the CERN data prefer the prediction of Oakes and Sakurai [23] $\theta = 28.2^\circ$.

(4) Because of the large difference between the CERN results and the Orsay (and DESY/M.I.T.) results, the average values of the data are not accurate enough to exclude the mass mixing models given by Kroll, Lee, Zumino [24]. In fact, the average values of the data are in remarkable agreement with the predictions of simple SU(3).

(5) The total widths of vector mesons determined directly from their leptonic decays are $\Gamma_\rho = 108.0 \pm 35$ MeV, $\Gamma_\omega = 14.0 \pm$ MeV, $\Gamma_\phi = 4.2 \pm 0.9$ MeV. These values are somewhat different from those obtained from the analysis of strong interaction experiments $\Gamma_\rho = 90-150$ MeV, $\Gamma_\omega = 12.2 \pm 1.3$ MeV, $\Gamma_\phi = 3.4 \pm 0.2$ MeV.

III. Photoproduction of Vector Mesons

(I) Motivation

Since photons and vector mesons have the same quantum numbers, it is very likely that at high energy and small momentum transfers the reaction $\gamma A \longrightarrow V^\circ A$ could have similar behavior as $\pi A \longrightarrow \pi A$, i.e., they should have the following characteristics:

(1) $\quad \dfrac{d\sigma}{dt} \sim \left| J_1(R\sqrt{-t}) \right|^2 \underset{t\ small}{\simeq} exp\left[\alpha(A,t)t\right],$ where a (A, t)

is a measure of nuclear density; its value depends sensitively on the t - range used and on A.

(2) As in the case of πp - scattering, the total cross section should be either slowly decreasing with increasing energy or be almost constant.

(3) For diffraction scattering, the produced vector mesons carry the same polarization as the initial photons. Thus the angular distribution of the decay K-pairs in photoproduction of ϕ mesons should be $\sim sin^2\theta^*$, where θ^* is the angle, in the ϕ rest system, between the decay K-meson and the recoil nucleus direction.

(4) To study the detailed mechanism by which vector mesons are produced at high energy and low momentum transfer on complex nuclei, we compare the data with the predictions of the diffraction models of Drell and Trefil, Ross and Stodolsky, Margolis, and Trefil, in which the forward production amplitude is expressed (in the laboratory system) as [25]

$$f_A = 2\pi f_H \int_{-\infty}^{\infty} dz \int_0^{\infty} b\,db\ e^{i\Delta\cdot b}\,e^{i\Delta_m\cdot z}\,\rho(z,b)\ exp\left(-\tfrac{\sigma}{2}\int_z^{\infty}\rho(z',b)\,dz'\right) \qquad (21)$$

where the factor $exp(i\Delta\cdot b)\rho(z,b)$ comes from nuclear shape, $exp(i\Delta_m\cdot z)$ comes from the difference in initial and final mass, $exp\left(-\tfrac{\sigma}{2}\int_z^{\infty}\rho(z',b)\,dz'\right)$ from the attenuation of the vector meson by nuclear matter after its production. $\sigma = \sigma_{VN}$ is the vector-meson-nucleon total cross section. The model of Drell-Trefil, Ross and Stodolsky assumes
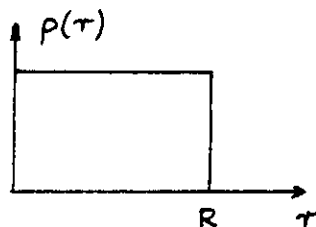
$$\rho(r) \begin{cases} = const & r \le R \\ = 0 & r > R \end{cases}$$

Thus the nucleus is treated in an average way as an absorbing medium, rather than as a collection of individual nucleons. Clearly, the model is best for nuclei in which A is large.

The Margolis model, based on approximate an summation of the multiple scattering series of Glauber, uses a Woods-Saxon distribution

$$\rho(r) = \rho_o \left(1 + exp[(r-c)/a] \right)^{-1}$$

for the nuclear density.

In the Margolis model terms 1/A and the effect of each individual vector meson nucleon scattering term $\frac{d\sigma}{dt} (\gamma p \rightarrow V p) = a \; exp \; (bt)$ is dropped. Thus the model is best for production on heavy nuclei at small momentum transfers, but will not apply to $A \leq 12$, when 1/A - terms are important.

The model of Trefil uses a density distribution

$$\rho(r) = \prod_{j=1}^{A} exp \left(-[r_j/R]^2 \right) \; ,$$

R = determined by rms nuclear radius.

This model keeps terms $\sim A^{-1}$ and b/R, and thus in principle should apply to all nuclei for both coherent and incoherent production.

For heavy nuclei at small momentum transfers there are very little differences between the three models above. The difference between the models occurs at large t or on small A.

In all three models, the following important properties are to be noted:

(A) To determine δ_{VN} one compares the relative yields $\frac{d\sigma}{d\Omega dm}(A_i) \Big/ \frac{d\sigma}{d\Omega dm}(A_j)$

for a set of nuclei (Be, C, Al, Cu, Ag, Ta, Pb) for a narrow mass band near the peak of the resonance so that the relative background contribution is small. Comparison of relative yields is the best way to determine δ_{VN} . It corresponds to the classical way of measuring total cross section with different target thickness.

(B) In principle, one can also determine δ_{VN} by matching the relative yields of

$$\frac{d\delta}{dt}\Big|_{t=0}(\gamma A \to A V^\circ) \Big/ \frac{d\delta}{dt}\Big|_{t=0}(\gamma p \to p V^\circ)$$

on each nucleus with

$$\left| f_A(R,t,\delta_{VN})/f_H \right|^2_{t=0}$$

In practice, however, there are some difficulties associated with this method:

(1) The function $\left| f_A(R,t,\delta_{VN}) \right|^2_{t=0} \sim R^4$, therefore the $\left| f_A/f_H \right|^2$ and the corresponding value δ_{VN} for large R depends critically on the nuclear radius parameters used. For example, as shown in the following figure taken from the calculation of Margolis and Koelbig[25] on the dependence of δ_{PN} on the ratio $\left| f_A/f_H \right|^2$, in the case of Pb an 8% change in nuclear radius would correspond to a change of δ_{PN} from 30 mb to 40 mb.
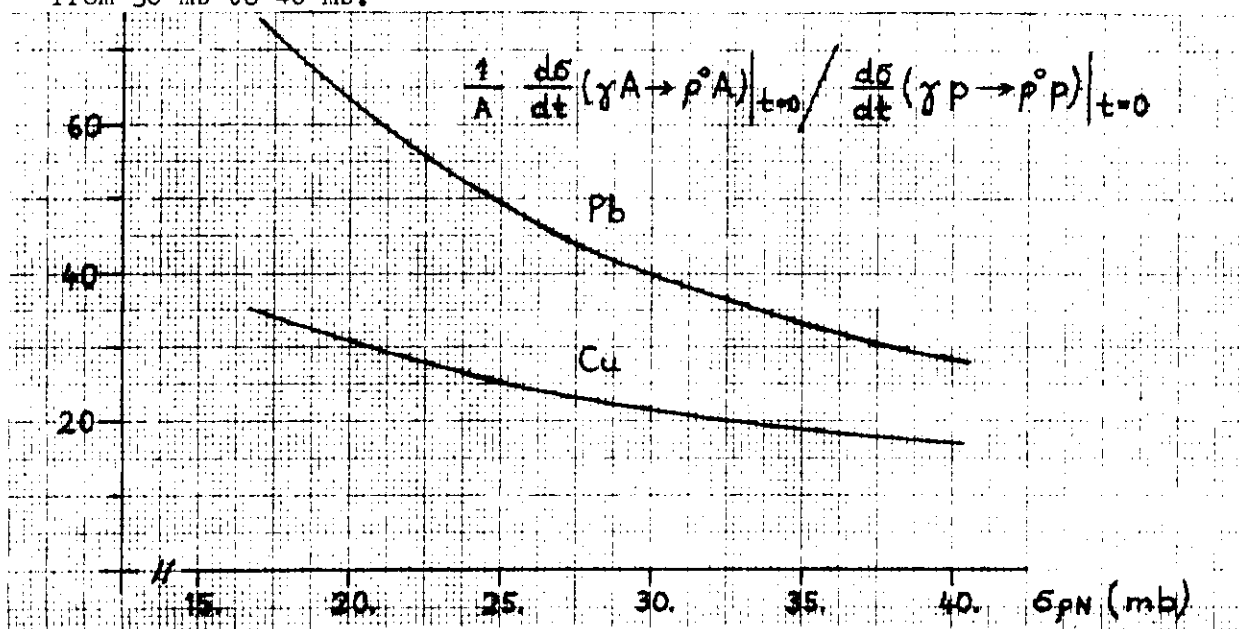
(2) For a wide resonance like the ρ meson, the absolute normalization of the experimental data cannot be accurate to more than $\simeq 25\%$. This is due to the fact that there is no reliable way to describe the shape of a wide resonance whose reported width varies between $\Gamma_\rho = 90$ and $\Gamma_\rho \mp 150$ MeV. The value Γ_ρ and thus the amount of pure ρ mesons in the observed $\pi^+\pi^-$ pairs depends sensitively upon the assumptions of Breit-Wigner form and background function. The two most commonly used methods are: The Soeding mechanism [26], whereby a photoproduced π pair is elastically scattered off the nucleus (diagram A). The interference between (A) and (B) below introduces a distortion in the resonance shape.
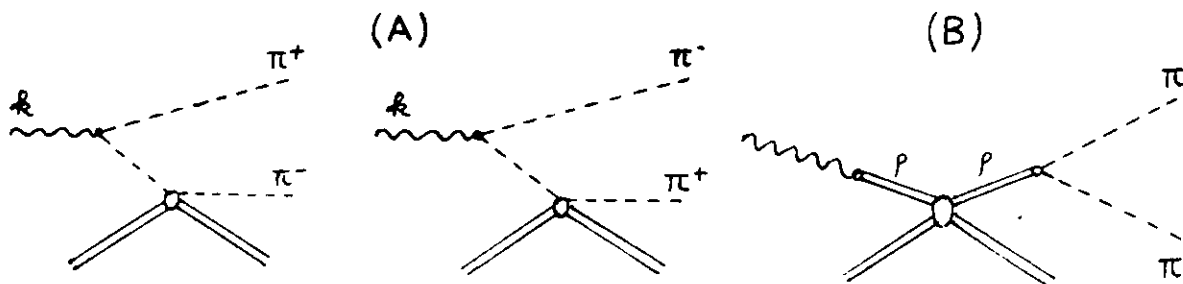
The Soeding mechanism not only cannot be calculated exactly, but also it constitutes serious double counting, since the $\pi^+\pi^-$ in diagram (A) must be in a p state in order to interfere with the pure p diagram (B). The method where one modifies the spectrum by a ($m_\rho / m_{\pi\pi}$)[4] factor (Ross and Stodolsky) [27] and uses an empirical background to fit the data, is also somewhat arbitrary, since the resultant cross section is somewhat dependent on the background function used.

Thus , depending on the method the data was analyzed, the ratio of the integrated cross section

$$\frac{\int_A \frac{d\sigma}{d\Omega\,dm}\,dm}{\int_H \frac{d\sigma}{d\Omega\,dm}\,dm} = \frac{\frac{d\sigma}{dt}\,(\gamma A \rightarrow A\rho^\circ)}{\frac{d\sigma}{dt}\,(\gamma P \rightarrow P\rho^\circ)}$$

can easily vary by 25% or more, as shown by the figure above.   In the case of Cu, a 25% variation in the ratio corresponds to a change of $\sigma_{\rho N}$ from 30 mb to 40 mb.

(C) With the knowledge of σ_{VN} , and with the assumption of pure imaginary scattering amplitude, one can now use the vector dominance model prediction, equation (8), or its equivalent term:

$$\frac{d\sigma}{dt}\Big|_{t=0}(\gamma A \rightarrow A V^\circ) = \frac{1}{16}\,\frac{\alpha}{4\pi}\left(\frac{\gamma_V^2}{4\pi}\right)^{-1}\sigma_T^2(V^\circ A) \tag{22}$$

to extract the value $\gamma_\rho^2/4\pi$ and compare it with the values obtained from π meson form factors, analysis of π^+, π^-, π° photoproduction etc. where the photon is also on the mass shell.

Since at finite energies the minimum momentum transfer $t = m_V^4/4k^2$ is far away from zero (typically on lead nucleus $d\sigma/dt \sim \exp(400\,t)$), the procedure of extrapolating $d\sigma/dt\big|_{t=0}$ from the measured $d\sigma/dt$ has all the difficulties (i.e. R[4] dependence, uncertainty in normalization, etc.) outlined above. These difficulties can be overcome [28], however, if one notes that in the optical model one has

$$\sigma_T(V^\circ A) = 4\pi \int_0^\infty b\,db\left[1 - \exp\left(-\sigma_{VN}\int_0^\infty \rho(b,z')\,dz'\right)\right] \sim R^2 \tag{23}$$

and if one now calculates $(d\sigma/dt)^{1/2}$ from eq. (21) with exactly the same set of density parameters R and $\rho(b,z)$ one has:

$$\left[\frac{d\sigma}{dt}(\gamma A \quad V^{\circ}A)\right]^{\frac{1}{2}} = 2\pi f_H \int_0^{\infty} b\,db \int_{-\infty}^{\infty} dz \; e^{i\Delta \cdot b} \; e^{i\Delta_m \cdot z} \rho(b,z) \exp\left(-\sigma_{VN}/2 \int_z^{\infty} \rho \, dz'\right)$$

$$\text{for } \Delta = 0 \quad = \frac{4\pi f_H}{\sigma_{VN}} \int_0^{\infty} b\,db \left(1 - \exp\left[-\sigma_{VN}\int_0^{\infty}\rho(b,z')\,dz'\right]\right) \sim R^2$$

(24)

Note that both $\sigma_T(V^{\circ}A)$ and $(d\sigma/dt)^{1/2}$ have the same functional dependence on R. Thus it follows from (22) that:

$$\frac{\gamma_p^2}{4\pi} = \frac{1}{16} \frac{\alpha}{4\pi} \frac{\sigma_T^2(V^{\circ}A)}{\frac{d\sigma}{dt}\Big|_{t=0}(\gamma A \rightarrow V^{\circ}A)} = \frac{1}{16}\frac{\alpha}{4\pi}\frac{\sigma_{VN}^2}{\frac{d\sigma}{dt}\Big|_{t=0}(\gamma p \rightarrow V^{\circ}p)} \qquad (25)$$

$$\text{independent of } R, \rho(b,z).$$

Therefore, the best way to obtain $\gamma_p^2/4\pi$ from photoproduction of vector mesons on nuclei is to determine σ_{VN} from <u>relative yields</u> for a set of nuclei in a narrow mass band near the peak of the resonance where the background is small and where no absolute normalization is necessary.

Using the σ_{VN} so obtained one then calculates $\sigma_T(V^{\circ}A)$ from (23) and extrapolates $d\sigma/dt\Big|_{t=0}$ from the measured total cross section $d\sigma/d\Omega$ with $|f_A(R,t,\sigma_{VN})|^2$———with exactly the same values for R and ρ (z). In this case it follows from the analysis of (25) that one has a unique $\gamma_p^2/4\pi$ independent of R and ρ (z).

For example with $d\sigma/dt_{t=0}$ (H) $= 150 \mu b/GeV^2$ one has:

(1) If the relative measurements yield a $\sigma_{pN} \cong 30$ mb then it follows from (25) $\gamma_p^2/4\pi \cong 0.5$ for all A.

(2) If the relative measurements yield a $\sigma_{pN} = 40$ mb then $\gamma_p^2/4\pi \cong 1.0$ for all A.

EXPERIMENTAL RESULTS:

I. <u>Photoproduction of ρ mesons:</u>

   a. <u>On hydrogen</u>

Large amounts of experimental data now exist on photoproduction of ρ on hydrogen, deuterium, and on complex nuclei.

The experiment of Ritson's group (SLAC, CIT, Santa Barbara, Northeastern Collaboration) [29] used a bremsstrahlung photon beam and a hydrogen target, and observed the recoiling protons produced i nthe target with a 90° bent spectrometer. The data were obtained by the photon subtraction technique. The results from 4 to 18 BeV are shown in Fig. 13. They are consistent with $d\sigma/dt = d\sigma/dt|_{t=0} \times \exp(Bt + Ct^2)$ with B = 8-10 GeV/c2.

The experiment of Mozley's [30] group at SLAC used a 2.2 meter streamer chamber to study the multibody photoproduction. A collimated bremsstrahlung beam of 16 GeV peak energy and 3 mm diameter was incident on a 3 atm hydrogen gas target extending through the chamber. The chamber was mounted on a large magnet with an8 kG field and triggered with a 4 fold coincidence array of scintillation counters.

The experiment of Silverman's [31] group at Cornell used a bremsstrahlung beam, scintillation counters and spark chambers to measure the positive and negative charged particles which traverse the spectrometer. The entire magnet system is mounted on a platform which rotates vertically about the target thus enabling them to vary the production angle.

Fig. 14 summarizes the results of $d\sigma/dt|_{t=0}$ from the above groups together with the results [32] from the DESY bubble chamber collaboration, the SLAC HBC group of Ballam, and the DESY counter group of Heinloth. As seen from the figure, the value $d\sigma/dt|_{t=0}$ decreases slowly with increasing energy, thus implying that $\sigma_{\rho p}$ also decreases with increasing energy. Fig.15 shows the summary of published values of $\sigma_{\rho p}$ from the various groups. These data show two interesting features:

A. At lower energies (2-3 GeV) the value $\sigma_{\rho p}$ depends, to $\simeq 25\%$, on the assumptions of fits, and

B. Within the errors the data are consistent with a slowly decreasing $\sigma_{\rho p}$ with increasing energy.

The DESY group of Criegee and Timm [33] has measured ρ production with polarized photons. Measurements with polarized photons provide a strong check on ρ production models. In a diffraction process (cross sections σ_1 in Fig. 16) the decay pions tend to emerge in a plane containing the polarization (electric) vector of the photon, while in 0^- exchange processes they come out perpendicularly. with cross sections σ_2 . This group has determined the ratio $R = \frac{\sigma_2}{\sigma_1}$ by measuring the $\pi^+\pi^-$ pairs on hydrogen with photons of two different polarizations. For photon energies between 2.0 and 2.5 GeV, and squared momentum transfers between -0.07 and -0.40, they find $R = 0.17 \pm 0.07$. This ratio indicates that ρ° photoproduction on hydrogen is dominated by the diffraction process. Since non-resonant π pairs have not been subtracted from the data, R represents an upper limit for non-diffractive ρ° production.

b) Onderline{On deuterium:}

Fig. 17 shows the summary of the data on deuterium from the DESY [32] bubble chamber collaboration and from Cornell [31]. The bubble chamber data agree with the coherent diffraction model calculation of Trefil with $\sigma_{\rho N} \simeq 30$ mb. The Cornell data exhibit coherence at small t-values. In the large t-region, the D_2 data have the same t-dependence as hydrogen and the ratio of cross sections $\frac{\sigma_d}{\sigma_p} \simeq 1.9$. The Cornell group also measured deuterium to hydrogen ratios at $\Theta = 0^\circ$, and as a function of E_γ. To an accuracy of about 5%, this ratio is independent of energy from 4 GeV to 9 GeV and averages to 2.87 ± 0.09. This ratio is different from the expected value of $\simeq 3.5$, based on coherent production and Glauber corrections. The Cornell result indicates that photoproduction of ρ on hydrogen cannot be completely diffractive.

c) Onderline{On complex nuclei:}

As discussed before, measuring ρ production on complex nuclei enables one to compare the relative yields with equation (21) and thereby obtain $\sigma_{\rho N}$. With the value $\sigma_{\rho N}$, one can then proceed to determine the coupling constant $\gamma_\rho^2/4\pi$ and compare the value with the analysis of other photoproduction data when the photon is on the mass shell.

The experiment done at DESY by the DESY-M.I.T. group [34] used a double arm spectrometer with mass resolution of $\pm$ 10 MeV. The relative yields were measured at 3 different energies of 2.7, 3.5, and 4.5 GeV. To reduce the background contribution, comparison with (21) was made at the central peak mass region between 720 and 820 MeV. The results shown in Fig. 18 yield an <u>average value</u> of δ_{pN} = 31.3 $\pm$ 2.3 mb for this energy region.

To obtain $\gamma_p^2/4\pi$, they integrated the forward cross section $\dfrac{d\delta}{d\Omega\,dm}$ over their spectrometer acceptances (3.0 $<$ p $<$ 6.2 GeV, 8° $<$ $\theta_{\pi\pi}$ $<$ 26°). They have also used an $(m_p/m_{\pi\pi})^4$ factor in their mass distribution to fit the spectrum. Their integrated cross sections over their acceptances are: $d\delta/d\Omega(C)$= 5.0 $\pm$ 0.4 mb/ sr-nucleon, $d\delta/d\Omega(Cu)$ = 11.2 $\pm$ 1.1 mb/sr-nucleon, $d\delta/d\Omega$(Pb) = 10.0 $\pm$ 1.0 mb/sr-nucleon.

From their spectrometer acceptance windows they then calculate an average value of $\left| f_A (R= 1.35\ A^{1/3}f,\ \delta_{pN} = 31\ \text{mb},\ t) \right|^2$ where each Monte Carlo event is weighted by the production mechanism of p. The values $\delta_{tot}(\gamma A)$ are again calculated using eq. (23) with the <u>same</u> R = 1.35 $A^{1/3}f$, δ_{pN} = 31 mb. From this information the values $\gamma_p^2/4\pi$ follow directly via:

$$\frac{\gamma_p^2}{4\pi} = \frac{\alpha}{4}\ \frac{k^2}{16\pi^2}\ \frac{\delta_T^2(R=1.35A^{1/3}f,\ \delta_{pN}=31mb)}{\frac{d\delta}{d\Omega}(A)\Big/\left|f_A(R=1.35\ A^{1/3}f,\ \delta_{pN}=31mb,\ t)\right|^2} \simeq 0.50 \pm 0.10$$

$$\text{for } C, Cu, Pb.$$

These numbers, as discussed before, depend only on δ_{pN} and the events/ acceptance, and are independent of any extrapolation procedure used. --- the R^4 factor cancels out in this case.

The experiment done at Cornell [31] used the spectrometer discussed previously. Their measured A-dependence of forward cross sections for E_γ = 6.0 GeV is also shown in Fig. 18. The curves in the figure are the optical model calculations for various assumptions about δ_{pN} . They used in their analysis the nuclear density distributions ρ (b, z) as given by Hofstadter for electron scattering. The value they obtained this way depends on A, being 30 mb for copper and 37 mb for lead. The authors attribute this dis-

crepancy to the neutron size being larger than the proton size.

It is clear from the published data that the values of δ_{pN} determined from DESY and Cornell do not contradict with each other.

To deduct $\gamma_p^2/4\pi$ the Cornell group proceeded in a manner quite different from the DESY method. They extrapolated the value $d\delta/dt|_{t=0}$ with the function $\left| f_A(t, \bar{R} = \text{electromagnetic radius}, \delta_{pN} = 40 \text{ mb}) \right|^2$. For $\delta_T(pA)$ they used the published values of Bellettini et al. on proton nucleus total cross sections, ie., they take $\delta_T(pA) = \delta(pA)$. In this way by extrapolating the ratio $\delta^2(pA)/(d\delta/dt, t=0)$ to $A \rightarrow \infty$ they obtained a value $\gamma_p^2/4\pi = 1.05 \pm 0.20$.

It is interesting to note that if one uses $\delta_T(pA) = \delta(nA)$ in the Cornell analysis, i.e., if one takes the measured values from Longo [35] et, al, or from Pontuev et. al, on neutron-nucleus total cross section and thus avoids the difficult problem of subtracting the Coulomb interference term from proton-nucleus total cross sections, then the value of $\gamma_p^2/4\pi (A \rightarrow \infty)$ is much closer to the results obtained from six or more other ways under similar kinematic conditions when the photon is on the mass shell (Fig.19).

The experiment of Leith's [36] group is one of the first successful coincidence experiments done on the 20 BeV SLAC. They used a large acceptance wire spark chamber spectrometer and a 9 BeV monochromatic photon beam to study the photoproduction of ρ on hydrogen and complex nuclei (Fig. 20). The resolution of the monochromatic peak is $\simeq \pm 1.5\%$. The spectrometer itself consists of a wide aperture, uniform field magnet, followed by a set of trigger counters and four wire spark chambers interfaced on-line with an IBM 1800 computer. Fig. 18 shows the result of their preliminary analysis on the relative yields of ρ on complex nuclei. The data are consistent with $20 \leq \delta_{pN} \leq 40$ mb. Using the assumption $\delta_T(pA) = \delta(pA)$, and not extrapolating to $A \rightarrow \infty$, they obtain an average value $\gamma_p^2/4\pi = 1.2 \pm 0.3$.

An experiment on electroproduction of ρ° was done at DESY by the Heinloth [37] group. The energy of the primary electron was 4.9 GeV, the energy of the virtual photon varied between 2.7 and 4.0 GeV. The momentum transfer was $|q^2| < 0.3$ GeV/^{2}. The result agrees with a Breit-Wigner $\times (m_\rho / m_{\pi\pi})^4$ distribution function and its t-dependence agrees well with the predictions of vector dominance.

The following table summarizes [38] some of the results of various ways of determining the coupling constant $\gamma_\rho^2 / 4\pi$.

ρ MESON ON MASS SHELL

Reactions	$\gamma_\rho^2/4\pi$
$e^+ + e^- \rightleftarrows \rho^\circ$	$0.52 \begin{array}{c} + 0.07 \\ - 0.06 \end{array}$

PHOTON ON MASS SHELL

	Reactions	$\gamma_\rho^2/4\pi$
1.	$\sigma_T^2(\gamma P) / \dfrac{d\sigma}{dt}(\gamma p \rightarrow \rho^\circ p)$	0.5 ± 0.1
2.	π meson form factor	0.53 ± 0.04
3.	$\gamma p \rightarrow \pi^+ n$, $\gamma n \rightarrow \pi^- p$ from 3 to 8 GeV	0.45 ± 0.10
4.	π^+/π^- ratio from deuterium	0.45 ± 0.10
5.	$d\sigma/dt(\gamma A \rightarrow \rho^\circ A)$ C, Cu, Pb DESY	0.5 ± 0.1
6.	$\Gamma(\omega \rightarrow \pi\gamma)/\Gamma(\omega \rightarrow 3\pi)$	0.65 ± 0.10
7.	$\dfrac{d\sigma}{dt}(\gamma p \rightarrow \pi^\circ p)/\dfrac{d\sigma}{dt}(\pi N \rightarrow \rho_\perp N)$	~ 0.5
8.	$\dfrac{d\sigma}{dt}(\gamma p \rightarrow \pi^+ n)$ vs. $\dfrac{d\sigma}{dt}(\pi^- p \rightarrow \rho^\circ n)$ [38]	0.45 (for this comparison see Fig. 21)
9.	$d\sigma/dt(\gamma A \rightarrow \rho^\circ A)$ Cornell	1.05 ± 0.20

IN/DIRECT MEASUREMENTS

1.	$\Gamma(\phi \rightarrow K^+ K^-)$	$\gamma_\rho^2/4\pi$ equiv.	$= 0.45 \pm 0.10$
2.	$\Gamma(K^* \rightarrow K\pi)$ etc.	$\gamma_\rho^2/4\pi$ equiv.	$= 0.6 \pm 0.1$

It is important to observe that the coupling constant $\gamma_p^2/4\pi = 0.5$ determined from direct measurements of leptonic decays of ρ when the ρ meson is on the mass shell is almost identical to that determined from various other measurements when the photon is on the mass shell.

The idea that the coupling constant varies slowly with q^2 seems to be quite valid.

II. Photoproduction of ω mesons:

For photon energies $2.1 < E_\gamma < 5.8$ GeV. The result of the DESY $^{(32)}$bubble chamber collaboration is shown in Fig. 22. The cross section for $\gamma p \longrightarrow p\omega$ can be described in the following form as a function of E_γ:

$$\sigma(\gamma p \longrightarrow p\omega) = (18.4 \pm 5.8) \ast E_\gamma^{-1.6} + (1.9\pm0.9) E_\gamma^{-0.08} \mu b$$

This expression was chosen because it is the behavior expected for the sum of two production mechanisms : 1) One meson exchange $\sim E_\gamma^{-1.6}$, 2) diffraction production $\sim E_\gamma^{-0.08}$. Thus below 3 GeV photoproduction of ω is dominated by one meson exchange where as at higher energies it is dominated by the diffraction mechanism.

III. Photoproduction of ϕ mesons:

a. On protons:

Fig. 23 shows the summary of the results from Ritson's $^{(29)}$ group at SLAC, from the DESY $^{(32)}$ bubble chamber group at lower energies (2.5 to 5.8 GeV), and the result from the DESY-M.I.T. $^{(34)}$ group at E_γ = 5.2 GeV and t $\simeq$ 0.

The Ritson data and the bubble chamber data both yield a slope $\frac{d\sigma}{dt} \sim \exp (5\ t)$. The DESY-M.I.T. data is consistent with this. But it is also consistent with a higher slope, say $\exp (8\ t)$. The bubble chamber data can be summarized as $d\sigma/dt = (1.6 \pm 0.6) \exp ([3.5 \pm 0.9]\ t)\mu b/ \text{GeV}^2$ with the integrated cross sections: σ_ϕ (2.5 - 3.5 GeV) = $(0.41 \pm 0.14)\mu b$, σ_ϕ (3.5 - 5.8 GeV) = $(0.45 \pm 0.13)\mu b$.

In analyzing the ϕ production data on hydrogen it is important to note that the competing reaction $\gamma p \rightarrow p + \phi + \pi^+ + \pi^-$ has a total cross section $\sigma_T (3.5 - 4.5) = (0.2 \pm 0.1)\mu b$, $\sigma_T (4.5 - 5.8) = (0.6 \pm 0.2)\mu b$. This makes the analysis of counter experiments with bremsstrahlung beams difficult.

b. On complex nuclei:

The DESY-M.I.T. group[34] has just completed an experiment studying the reaction

$$\gamma + A \rightarrow A + K^+ + K^- \qquad (26)$$

at an incident photon energy of 5.2 GeV on targets of Be, C, Al, Cu, Ag, Ta, and Pb. They detected the $K^+ K^-$ pairs with 4 large aperture Cerenkov counters and with hodoscopes in the spectrometer to provide a mass resolution of $\pm$ 5 MeV. A total of 20,000 $K^+ K^-$ events was observed. The $K^+ K^-$ mass spectra from Be, C, Al, Cu, Ag, Pb are shown in Fig. 24. The mass resolution of the hodoscope system has not been unfolded. The errors in the figures 24 and 25 are statistical only. An additional normalization uncertainty of $\pm$ 16% is not included.

As seen from Fig. 24, in the $K^+ K^-$ invariant mass region 1000 to 1085 MeV/c^2, reaction (26) is dominated by ϕ-meson production. Within the statistical accuracy, no other enhancements were observed.

To study the mechanism by which ϕ-mesons are produced at high energy and low momentum transfer, they compare the data with the predictions of the diffraction models of Drell and Trefil, Ross and Stodolsky, Margolis, and Trefil, in which the forward production cross section is expressed (in the laboratory system) as $d\sigma/d\Omega(total) = d\sigma/d\Omega(coherent) + d\sigma/d\Omega$ (incoherent),

$$d\sigma/d\Omega \text{ (coherent) } = C (A)p^2 \left| f_A (R, t, \sigma_{\phi N}) \right|^2 \qquad (2)$$

where p is the momentum of the ϕ meson, R is a set of parameters which describe the nuclear density distribution, t is the square of the momentum transfer to the nucleus, and C (A) is a normalization constant. The coherent cross section includes those reactions in which the nucleus remains in its ground state, while the incoherent cross section includes reactions in which the nucleus is excited or fragmented. The function $f_A (R, t, \sigma_{\phi N})$ defined in (21) is chosen such that $\left| f_A (R, 0, \sigma_{\phi N}) \right|^2 = 1$.

By measuring $d\sigma/d\Omega$ as a function of A, t, and p, one can compare the experimental data to the different theories of production, and determine the value of $\sigma_{\phi N}$.

The results of these comparisons are as follows: (They restrict the analysis to the mass region 1016 < m < 1025 MeV/c^2 as defined in Fig. 24).

a) A - dependence

The cross section $d\sigma/d\Omega \left(\Theta_\phi < .5^\circ \right)$ was measured on targets of Be, C, Al, Cu, Ag, Ta, and Pb, at $\langle p \rangle$ = 5.2 GeV/c. The relative cross sections $\dfrac{1/A \cdot d\sigma/d\Omega (A)}{1/9 \cdot d\sigma/d\Omega (Be)}$, normalized to Be, are shown in Fig. 25a. The A-dependence of the production cross section yields information on the mean free path in nuclear matter. To obtain $\sigma_{\phi N}$ the data were first corrected for contributions from non-resonant background and incoherent production. The background ($\sim 5\%$) was subtracted by matching a Monte Carlo calculation of the non-resonant mass spectra to the data outside the peak. The incoherent contribution to $\dfrac{d\sigma}{d\Omega}$ was estimated using the model of Trefil by calculating the difference between the cross section summed over all nuclear states and the cross section due to the ground state only. For the heavier elements, this agrees with the same calculation from the model of Margolis . The determination of $\sigma_{\phi N}$ was carried out using three different theoretical models. The measured coherent production cross section was matched both to the Drell-Trefil model, using a step function density distribution to describe the nucleus, and to the Margolis model, using a Wood-Saxon density distribution. The data without incoherent subtraction were also matched to the model of Trefil.

The best value of $\sigma_{\phi N}$ is then .

$$\sigma_{\phi N} = (12.0 \pm 3.9) \text{ mbarn}$$

There is no significant difference in the value of $\sigma_{\phi N}$ obtained from different theories of nuclear photoproduction. The value of $\sigma_{\phi N}$ is to be compared with the quark model prediction of Joos[8] $\sigma_{\phi N}$ = 11 mbarn.

b) t - dependence

The typical behavior of $d\sigma/dt$ as a function of 4-momentum transfer squared $t = (p-k)^2$ at a fixed central ϕ° laboratory momentum of 5.2 GeV/c is shown in Fig. 25b for the C target. In the t-region of this experiment $.009 < |t| < .016$ (GeV/c)^2 the data are fitted well by a form $d\sigma/dt \sim e^{at}$ with a = (58 ± 12) (GeV/c)$^{-2}$.

c) p - dependence

The behavior of $\dfrac{\langle p^2 \rangle \langle f_A^2 \rangle}{p^2 |f_A^2|} \dfrac{d\sigma}{d\Omega}$ as a function of p over a momentum range from 4.7 to 5.6 GeV/c is shown in Fig. 25c. The fit of this quantity to the data yields $\dfrac{\langle p^2 \rangle \langle f_A^2 \rangle}{p^2 |f_A|^2} \dfrac{d\sigma}{d\Omega} = (129.2 \pm 2.0) - (15.7 \pm 9.2)$ (p - 5.2). This quantity is relatively independent of p, consistant with $\dfrac{d\sigma}{d\Omega}$ varying as p^2 in agreement with the predictions of the diffraction model. However, due to the limited p range available, a small decrease in the total cross section with increasing p cannot be excluded.

d) ϕ - polarization

As a consistency check of the diffraction production of ϕ mesons, they show in Fig. 25d the angular distribution of the decay kaons in the ϕ° rest system. As seen, the data agree well with the distribution function

$$W_{KK}(\theta^*) = \frac{3}{8\pi} \sin^2\theta^*$$

(θ^* is the angle between decay products and the recoil target particle measured in the K$^+$K- CMS.) . The data show that the ϕ mesons produced are transversely polarized, which is consistent with the other evidence that they are produced via diffraction off the whole nucleus.

In Summary, the dependence upon p, t, and A of the high energy, small angle ϕ° photoproduction cross section is in agreement with the general

features of the diffraction model and the cross section can be expressed in the simple form

$$\frac{d\sigma}{d\Omega} = C(A)\, p^2 \, |f_A(R,t,\, \sigma_{\phi N})|^2 \underset{t \longrightarrow 0}{\simeq} C(A)\, p^2 \, e^{at}$$

The ϕ -nucleon cross section obtained in this experiment agrees well with the quark model predictions.

IV. Total Photon Hadron Cross Sections:

In the vector dominance model one can relate photoproduction cross sections of vector mesons with the vector meson nucleon cross sections, eq.(8). In particular, the total γp cross section can be expressed as:

$$\sigma_{tot}(\gamma p) = \sqrt{4\pi\alpha}\, \left[\left(\frac{\frac{d\sigma}{dt}\big|_{t=0}(\gamma p|\rho p)}{\gamma_\rho^2/4\pi} \right)^{\frac{1}{2}} + \left(\frac{\frac{d\sigma}{dt}\big|_{t=0}(\gamma p|p\omega)}{\gamma_\omega^2/4\pi} \right)^{\frac{1}{2}} + \left(\frac{\frac{d\sigma}{dt}\big|_{t=0}(\gamma p|p\phi)}{\gamma_\phi^2/4\pi} \right)^{\frac{1}{2}} \right]$$

Since $\frac{d\sigma}{dt}\big|_{t=0}(\gamma p|\rho p)$, $\frac{d\sigma}{dt}\big|_{t=0}(\gamma p|p\omega)$, $\frac{d\sigma}{dt}\big|_{t=0}(\gamma p|p\phi)$ are all

measured values, and since $\gamma_\rho^2/4\pi$, $\gamma_\omega^2/4\pi$, $\gamma_\phi^2/4\pi$ are determined from leptonic decays, measurement of $\sigma_{tot}(\gamma p)$ thus enables us to compare it directly with the prediction of the vector dominance model. This measurement provides the most direct confirmation that the coupling constants

$\gamma_\rho^2/4\pi$ etc. have almost the same values independent of whether the ρ or the photon is on the mass shell.

Two experiments were done on $\sigma_{tot}(\gamma p)$[32]. The one from S.L.A.C. was done at 7.5 GeV. The method used was to expose the S.L.A.C. $40''$ HBC to high energy positron-electron annihilation radiation, (plus a background of wide angle bremsstrahlung) and to subtract out the bremsstrahlung contribution by making an identical exposure using electron induced radiation instead of that from positrons. Their result is $\sigma_{tot}(\gamma p) = (151 \pm 24)\ \mu b$.

The DESY experiment was done on the 85 cm HBC. Using a tagged photon beam, they have measured the cross section from .5 GeV up to 5.0 GeV. Their result, together with the S.L.A.C. result, is shown in Fig. 26.

Also shown in Fig. 26 is the region predicted by the vector dominance model. As seen, the data agree well with the vector dominance model and provide an excellent consistency check on the interrelations of the various experimental numbers obtained so far.

V.   Upper limits - Rare Decays of Vector Mesons:

Finally, the following upper limits on rare decays of vector mesons are obtained:

From DUBNA: [39]
$$R_1 = \frac{N(\omega \to \eta\gamma)}{N(\omega \to \pi^\circ\gamma)} = .22 \pm .11$$

$$R_2 = \frac{N(\omega \to \pi^\circ\pi^\circ\gamma)}{N(\omega \to \pi^\circ\gamma)} = .25 \pm .15$$

From PISA: [40]
$$BR(\phi \to \pi^\circ\gamma) \leq 1.2 \times 10^{-2}.$$

Acknowledgments.

References

1. W.C. Barber, B. Gittelman, G.K. O'Neill, B. Richter.

2. U. Becker, W.K. Bertram, M. Binkley, K. Cohen, T.M. Knasel,
    R. Marshall, D. Quinn, M. Rohde, S.C.C. Ting.

3. W.W. Ash, K. Berkelman, C.A. Lichtenstein, R.M. Littauer,
    R.H. Siemann.

4. C. Bernardini, F. Felicetti, R. Querzoli, V. Silvestrini,
    G. Vignola, L. Meneghetti Vitale, S. Vitale, G. Penso.

5. For complete references see: S.C.C. Ting, Proceedings of the
    1967 International Conference on Photons and Electrons,
    Stanford, California, and J.J. Sakurai: Vector Mesons 1960-1968,
    University of Chicago Preprint EFI 68-59.

6. A. Dar and V.F. Weisskopf, Phys. Letters 26B, 670 (1968).

7. M. Gell-Mann, D. Sharp, and W.G. Wagner, Phys.Rev. Letters,
    8, 261 (1962).

8. H. Joos. Proceedings of 1967 International Conference on High
    Energy Physics, Heidelberg, Germany.

9. R.J. Oakes. Nuovo Cimento, Vol. XLIVA,N.2. P. 440 (1966).

10. R. Gatto. Proceedings of Hamburg Conference 1965.

11. J.K. de Pagter, J.I. Friedman, G. Glass, R.C. Chase, M. Gettner,
    E. von Goeler, R. Weinstein, and A.M. Boyarski, Phys.Rev.Lett.
    16, 35 (1966).

12. J.G. Asbury, W.K. Bertram, U. Becker, P. Joos, M. Rohde, A.J.S.
    Smith, S.C.C. Jordan, and Samuel C.C. Ting, Phys.Rev.Lett. 19,
    869 (1967).

13. A.Wehmann, E. Engels, L.N. Hand, C.M. Hoffman, P.G. Innocenti,
    Richard Wilson, W.A. Blanpied, D.J. Drickey, D.G. Stairs.Contri-
    bution to this conference.

14. V.L. Auslander, G.I. Budker, Ju. N. Pestov, V.A. Sidorov, A.N.
    Skrinsky, A.G. Khabakhpashev. Contribution to the conference.

15. J.E. Augustin, J.C. Bizot, J. Buon, J. Haissinski, D. Lalanne, P.C. Marin, H. Nguyen Ngoc, J. Perez-Y-Jorba, F. Rumpf, E.Silva, S. Travernier; Contribution to the Conference.

16. U. Becker, W.K. Bertram, M. Binkley, C.L. Jordan, T.M. Knasel, R. Marshall, D. Quinn, M. Rohde, A.J.S. Smith, and Samuel C.C.Ting; Contribution to this Conference.

17. J.E. Augustin, J.C. Bizot, J. Buon, B. Delcoart, J. Haissinski, J. Jeanjean, D. Lalanne, P.C. Marin, H. Nguyen Ngoc, J. Perez-Y-Jorba, F. Richard, F. Rumpf, D. Treille.

18. D. Bollini, A. Buhler-Broglin, P. Dalpiaz, T. Massan, F.Navach, F.L. Navarria, M.A. Schneegans, and A. Zichichi; Contributions to the Conference.

19. J.E. Augustin, D. Benaksas, J. Buon, U. Gracco, J. Haissinski, D. Lalanne, F. LaPlanche, J. Lefrancois, P. Lehmann, P. Marin, F. Rumpf, E. Silva; Contribution to the Conference.

20. R.G. Astvakaturov, M.A. Azimov, A.M. Baldin, A.S. Belousov, I.V. Chuvilo, J.Hladky, U.I. Ivanov, M.N. Khachaturyan, M.S. Khuastunov, A.I. Manyushin, L.N. Shtarkov, L.I. Zhuravleva.

21. D.M. Binnie, A. Duane, A.R. Farugui, P.J. Horsey, M.G. Jones, M.E. Kay, D.C. Mason, P.J. Nicholson, I.U. Rahman, J. Walters, and J.G. Wilson.

22. T. Das, V.S. Mathur, S. Okubo , Phys. Rev. Letters $\underline{19}$, 470 (1967).

23. R.J. Oakes, and J.J. Sakurai: Phys. Rev. Letters $\underline{19}$, 1266 (1967).

24. N. Kroll, T.D. Lee, and B. Zumino: Phys. Rev. $\underline{157}$, 1376 (1967).

25. S.D. Drell and J.S. Trefil, Phys.Rev. Letters $\underline{16}$, 552 and 832 (E) (1966), and M.Ross and Stodolsky, Phys. Rev. $\underline{149}$, 1172 (1966), K.S. Koelbig, and B. Margolis, CERN preprint 68/482/5 (1968), and J.S. Trefil, MIT (CTP-15, to be published).

26. P. Soeding, Phys.Letters $\underline{19}$, 702 (1965).

27. M. Ross and L. Stodolsky, Phys.Rev. 149, 1172 (1966).

28. U. Becker, and J.S. Trefil; Contribution to the Conference.

29. W.G. Jones, K. Kreinick, R. Anderson, D. Gustavson, J. Johnson, and D. Ritson, F. Murphy, M. Gettner, and R. Weinstein. Contribution to the Conference.

References - cont'd

30. M. Davier, I. Derado, D. Drickey, D. Fries, R. Mozley, A. Odian, F. Villa, D. Yount, and R. Zdanis; Contribution to the Conference.

31. G. McClellan, N. Mistry, P. Mostek, H. Ogren, A. Silverman, J.Swartz, R. Talman; Contribution to the Conference.

32. Aachen-Berlin-Bonn-Hamburg-Heidelberg-Muenchen-Collaboration - Contribution to the Conference.
J. Ballam, G.B. Chadwick, Z.G.T. Guiragossian, P.Klein, A. Levy, M.Menke, E. Pickup, T.H. Tan, and G. Wolf - Contribution to the Conference. H. Blechschmidt - DESY Report 1967.

33. L. Criegee, M.H.Garrell, C. Gottfried, A. Krolzig, G. Loeffler, K.P. Schueler, U. Timm, W. Zimmermann, H. Werner, G.P. Collins, P.W. Dougan, E. von Goeler, and R.A. Carrigan, Contribution to this conference.

34. J.G. Asbury, U. Becker, W.K. Bertram, P. Joos, M. Rohde, A.J.S.Smith, C.L. Jordan, and Samuel C.C. Ting. Contributions to the Conference.

35. M.J. Longo et al.; Proceedings of Conference on High Energy Conference, CERN, 1968, Vol. I, P. 523. V.S. Pantuer et al. , JETP 15, 626 (1962), J. Exptl. Theoret. Phys. 42, 909 (1962).

36. F. Bulos, W. Busza, R. Diebold, R. Giese, R.R. Larsen, D.W.G.S. Leith, B. Richter, R. Russell, L. Kauffman, V.Perez-Mendez, A. Stetz, S.H. Williams, M. Beniston, J. Rettberg.

37. H. Blechschmidt, J.P. Dowd, B. Elsner, K. Heinloth, P. Karow, J.Rathje, D. Schmidt, J.H. Smith, A. Kanaris, A.G. Wynroe; Contribution to the Conference.

38. J.J. Sakurai; Contribution to the Conference.
Ivan Derado, Z.G.T. Guiragossián; Contribution to the Conference.
A. Dar, V.F. Weisskopf, C.A. Levin-son, H.J. Lipkin, P.R.L. 20, 1261 (1968).
R. Diebold, J.A. Poirer, P.R.L. 20, 1532 (1968), etc.

39. Strugalski et al (DUBNA). Contribution to the Conference.

40. P. Braccini, L. Foa, K. Luebelsmeyer, D. Schmitz, Contribution to the Conference.

Figure captions:

Fig. 1   Apparatus and brief review of the Princeton - Stanford
          e^+e^- scattering experiment.

Fig. 2   The Feynman diagrams, the apparatus, and the results of the
          DESY - M.I.T. wide angle electron pair production experiment.

Fig. 3   The Feynman diagrams, the apparatus, and the results of the
          experiment on wide angle bremsstrahlung by Ash, Berkelman,
          et al.

Fig. 4   Summary of the results of the pair production and wide angle
          bremsstrahlung experiments.

Fig. 5   Invariant mass spectra on $\rho \rightarrow \ell^+\ell^-$ from DESY-M.I.T. and
          from Harvard. The $\rho \rightarrow \pi^+\pi^-$ spectra measured by the DESY-
          M.I.T. group under the same kinematical conditions are also
          shown.

Fig. 6   Summary of characteristics of various storage rings.

Fig. 7   Experimental set-up and results on $e^+e^- \rightarrow \rho \rightarrow \pi^+\pi^-$ from ORSAY.

Fig. 8   Invariant mass spectra of $\phi \rightarrow e^+e^-$ and $\phi \rightarrow K^+K^-$ measured
          in the same apparatus, by the DESY-M.I.T. group.

Fig. 9   Experimental results on $\omega \rightarrow e^+e^-$ and $\phi \rightarrow e^+e^-$ from
          the Zichichi group at CERN.

Fig. 10   Experimental results on mass spectra of $e^+e^- \rightarrow \omega \rightarrow \pi^+\pi^-\pi^o$ from
          ORSAY.

Fig. 11   Experimental set-up and results on leptonic decays of vector
          mesons from the Baldin group at Dubna.

Fig. 12   Comparison of the world average on leptonic decays of vector
          mesons with Weinberg's first sum rule.

Fig. 13   Experimental results from the Ritson group at S.L.A.C.
          $\frac{d\sigma}{dt}$ in (GeV/c)^2 versus t, for the reaction $\gamma + p \rightarrow p + \rho^o$
          at incident photon energies from 6.5 GeV to 17.8 GeV. The lines
          drawn through the data points are the best fits to the expres-
          sion $\frac{d\sigma}{dt} = A\,e^{Bt+Ct^2}$. The values of A, B and C found at each
          energy are shown in the figure. Their units are $\mu b/(GeV/c)^2$,
          $(GeV/c)^{-2}$, and $(GeV/c)^{-4}$ respectively.

Figure captions - cont'd

Fig. 14   Summary of $\frac{d\sigma}{dt}\big|_{t=0}(\gamma p \to p\rho^\circ)$. The decreasing of this
value with increasing photon energy indicates that δ_ρ decreases
slowly with energy.

Fig. 15   Summary of total cross section $\sigma_{tot}(\gamma p \to p\rho^\circ)$. Note that in the
low energy region, $E_\gamma \leq 4$ GeV, the value σ_{tot} depends sensitive-
ly on the method of analysis used.

Fig. 16   Experimental results of the photoproduction of the ρ meson on
protons with polarized photons, at an energy of 2.2 GeV. See
text for further explanation.

Fig. 17   Summary of photoproduction of ρ mesons on deuterium. The straight
lines on the $d\sigma/dt$ plot are the predictions of the diffraction
model of Trefil. See text for details.

Fig. 18   Summary of relative yields of production of ρ mesons on complex
nuclei from measurements at DESY at photon energies of 2.7, 3.5,
and 4.5 GeV, from Cornell at 6 GeV, and from S.L.A.C. at 9 GeV.
See text for explanation of the solid curves.

Fig. 19   Comparison of the coupling constant $\gamma_\rho^2/4\pi$ determined from the
DESY analysis and from the Cornell analysis. The solid line is
the result of the Cornell analysis if one replaces $\delta_{\rho A}$ with
the two results of δ_{nA} . The region between the dotted lines
is determined from various other analyses of experiments where
the photon is on the mass shell.

Fig. 20a   Schematic drawing of the S.L.A.C. (Leith) spectrometer.
Fig. 20b   Energy spectrum of the annihilation beam as measured in the pair
spectrometer mode $\gamma + Al \longrightarrow Al + e^+ + e^-$.

Fig. 21   Comparison of the vector dominance model by Derado and Guragossián.
The ▲ are the predicted $\gamma p \to n\pi^+$ cross sections using the
measured $\pi^- p \to n\rho^\circ$ cross sections and the vector dominance
model. The O are the experimental results on $\gamma p \longrightarrow n\pi^+$
from Boyarski et. al. at S.L.A.C. The agreement is good.

Figure captions - cont'd

Fig. 22   Total cross section for $\gamma + p \longrightarrow p + \omega$ from the DESY
            bubble chamber group.

Fig. 23   Invariant mass spectra of the reaction $\gamma + p \longrightarrow p + \phi$ from
            the DESY-M.I.T. group and summary of the data on $d\sigma/dt$
            $(\mu b/GeV^2)$ versus t from S.L.A.C. and DESY.

Fig. 24   Kaon pair invariant mass spectra $d\sigma/d\Omega\, dm$
            $(\mu b/sr \cdot nucleon \cdot MeV/c^2)$ at $\langle p \rangle$ = 5.2 GeV/c for target
            nuclei of Be, C, Al, Cu, Ag, Pb. The dotted lines are the esti-
            mates of the non-resonant background contributions. The solid
            curves are the $\phi \rightarrow 2K$ mass distribution produced via a Monte
            Carlo program which generated ϕ mesons $(m_\phi = 1019.5\ MeV,$
            $\Gamma_\phi = 3.4 MeV)$ at the target).

Fig. 25a   Dependence of $d\sigma/dt$ upon A, the atomic number of the target.
            The results are shown for average ϕ momentum p = 5.2 GeV/c.
            The crosses are best fit points to the model of Drell-Trefil.

Fig. 25b   The typical behavior of $d\sigma/dt$ is shown as a function of t,
            the square of momentum transfer to the nucleus, for a carbon
            target. The solid curve is the best fit to $e^{\alpha t}$.

Fig. 25c   The behavior of $\dfrac{\langle p^2 \rangle \langle f_A^2 \rangle}{p^2\,|f_A|^2} \cdot \dfrac{d\sigma}{d\Omega}$ as a function of p. To a
            good approximation, the cross section $d\sigma/d\Omega$ is propor-
            tional to p^2. (See text for details).

Fig. 25d   The angular distributions of the decay kaons in the $\phi^0 -$
            rest system. θ^* is the angle between the decay products and
            recoil target particle in the ϕ -CMS. As seen, the data agree
            well with the $sin^2\theta^*$ distribution function.

Fig. 26   Summary of experimental results on total hadronic cross-sections
            from DESY and from S.L.A.C. The shaded region is then prediction
            of the vector commance model (Eq. 27).

Princeton - Stanford - Exp.
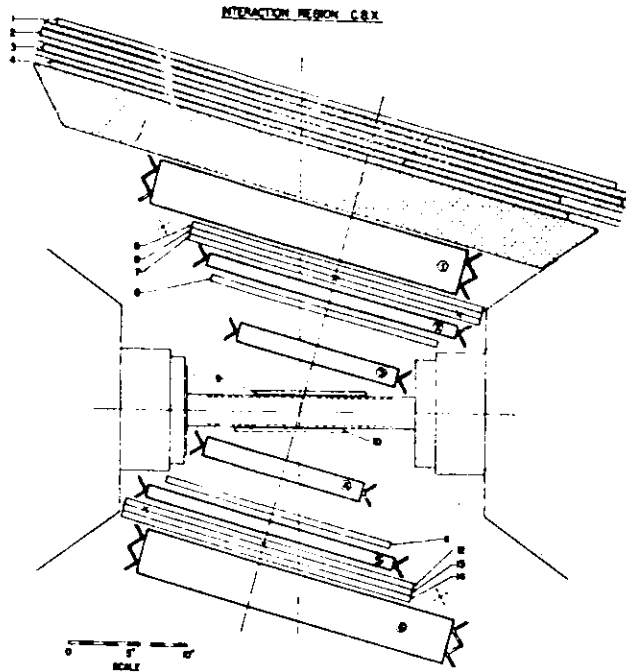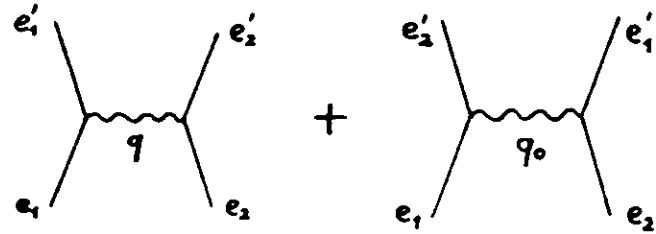
INTERACTION REGION C8X

$e^- + e^- \longrightarrow e^- + e^-$

$$\frac{d\sigma}{d\Omega}(\theta, \kappa) = \frac{r_0^2}{8}\left(\frac{m}{E}\right)^2\left[\frac{s^4 + q_0^4}{q^4}G_\kappa^2(q^2)\right.$$

$$\left. + \frac{2s^4}{q^2 q_0^2}G_\kappa(q^2)G_\kappa(q_0^2) + \frac{s^4 + q^4}{q_0^4}G_\kappa^2(q_0^2)\right](1+\delta)$$

$$s^2 = 4E^2 \quad , \quad G_\kappa(q^2) = \left(1 - \frac{q^2}{\kappa^2}\right)^{-1}$$

$$\frac{1}{\kappa^2} = 0 \implies G_\kappa(q^2) = 1 \implies \text{point-like}$$

electron $\implies$ no cut-off for photon propag.

Results: Based on 7000 events:

$$\frac{1}{\kappa^2} = (-.06 \pm .06)(\text{GeV/c})^2$$

consistent with $\frac{1}{\kappa^2} = 0$

Fig.1

DESY-MIT WIDE ANGLE PAIR PRODUCTION

Fig. 2

Berkelman et al.

$t^2 = (p_2 + k)^2 > 0$

time-like

$q^2 = (p_1 - k)^2 < 0$

space-like

Compton - term

small (few %)

$R = 0.94 \pm 0.14 + (0.9 \pm 1.9) \cdot 10^{-4} M$

Mass Of Final State (MeV/c^2)

Fig. 3

Fig. 4

DESY — M.I.T.

$\gamma C \rightarrow C \rho^\circ$
$\downarrow \pi^+\pi^-$

CROSS SECT.

M_{xx} [MeV/c^2]

CROSS SECT.

$\rho^\circ \rightarrow e^+ e^-$

$\begin{cases} m = 765\ \text{MeV/c}^2 \\ \Gamma = 130\ \text{MeV} \end{cases}$

$M_{e^+e^-}$ [MeV/c^2]
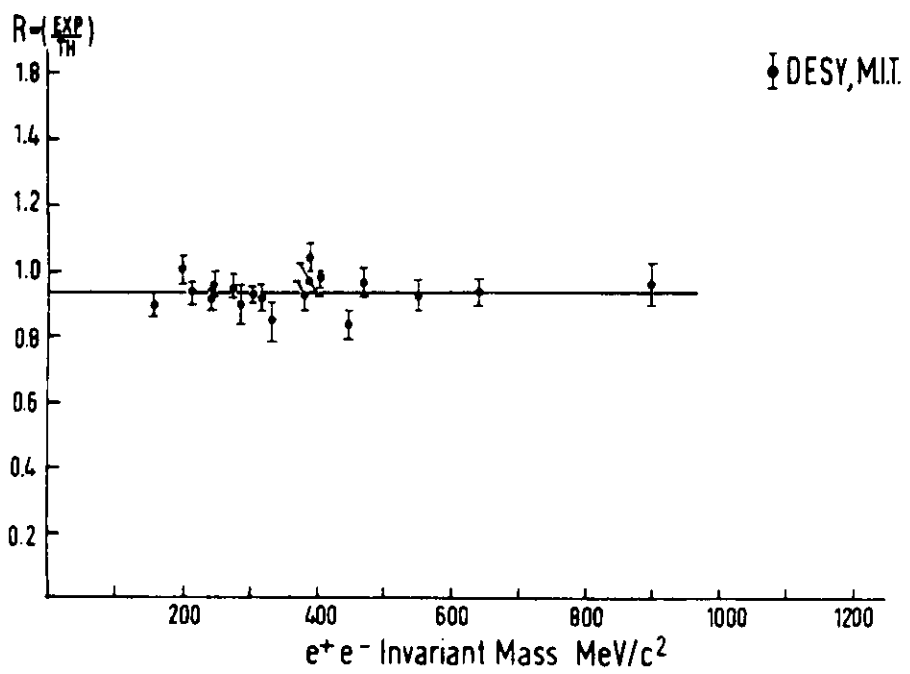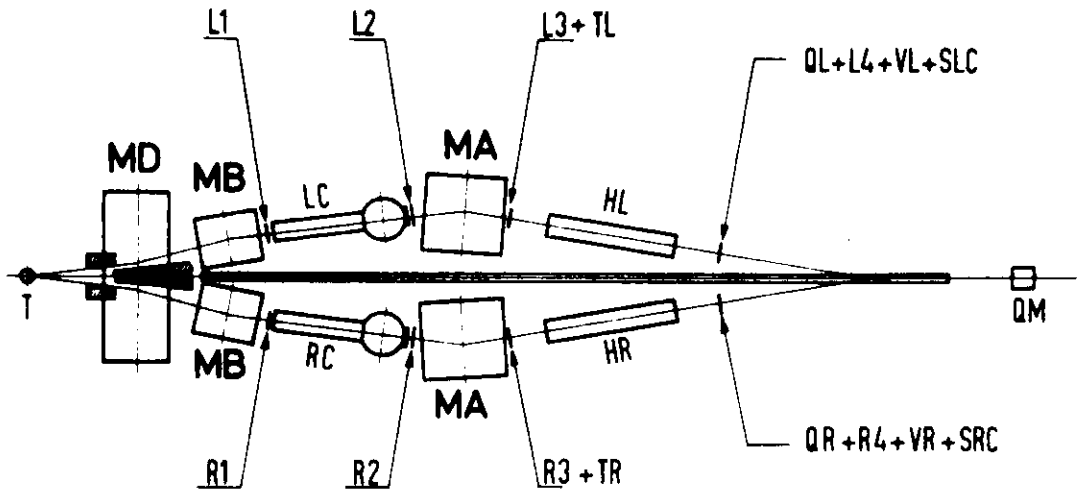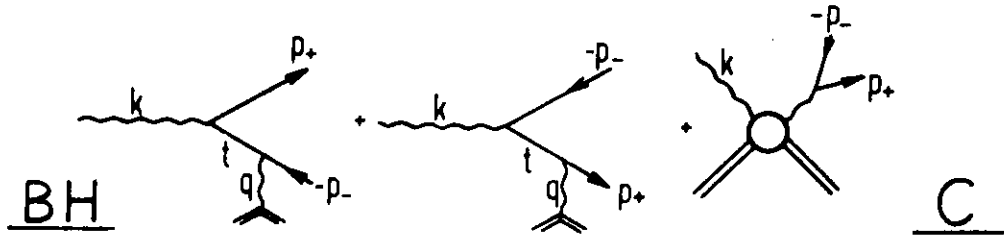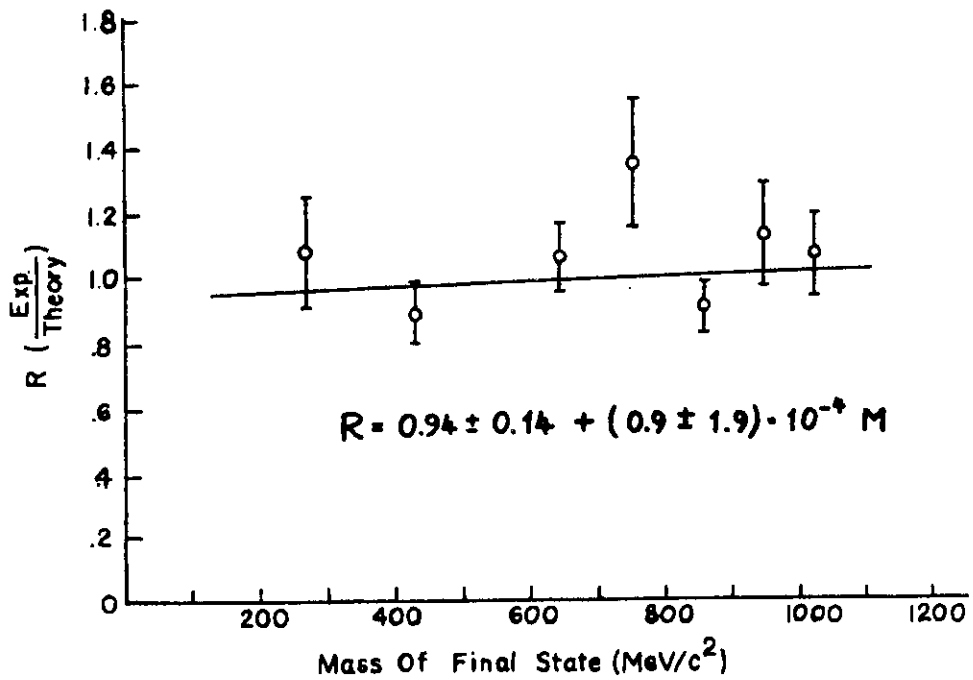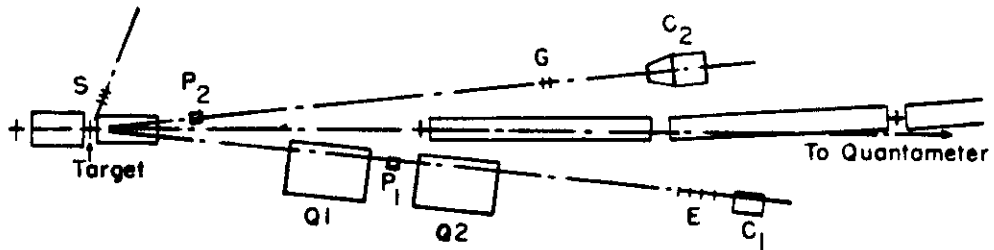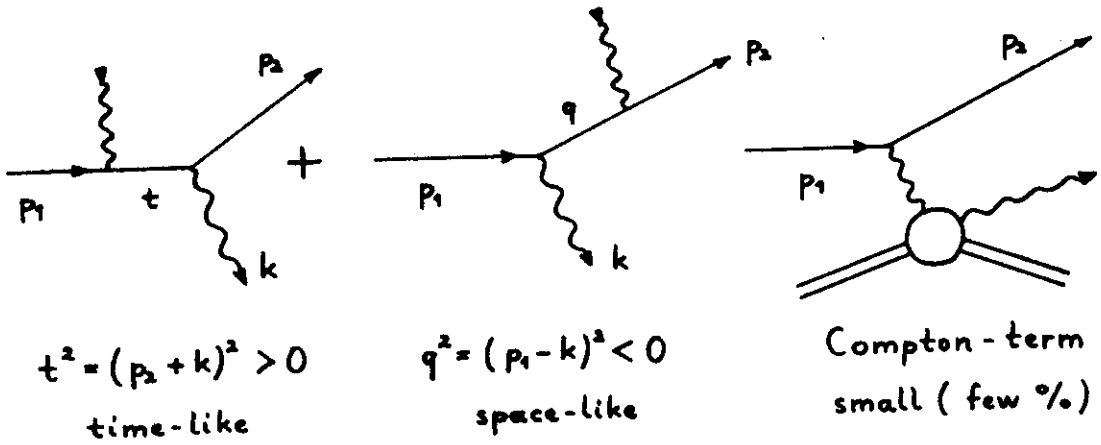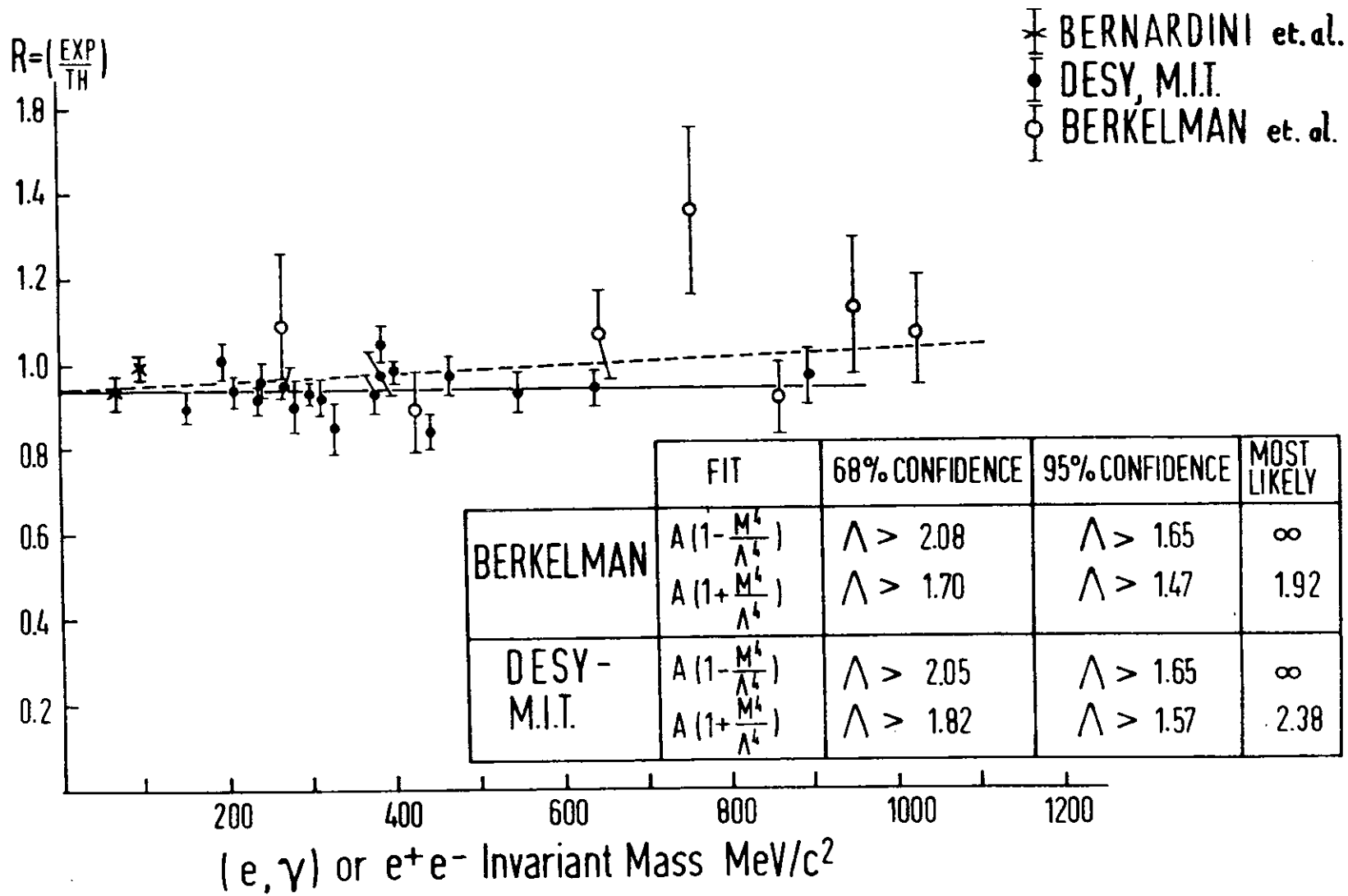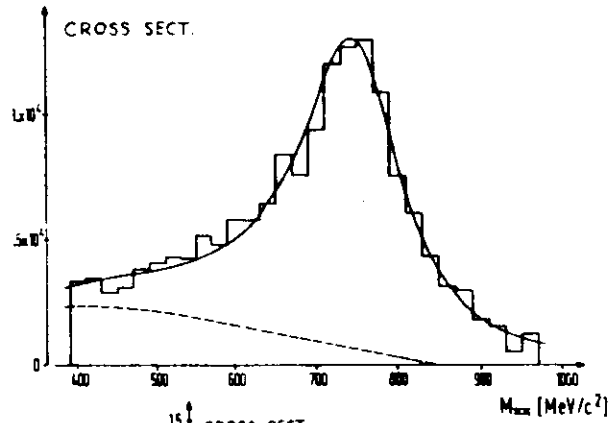
BR =

(6.4 ± 1.5)

× 10^{-5}
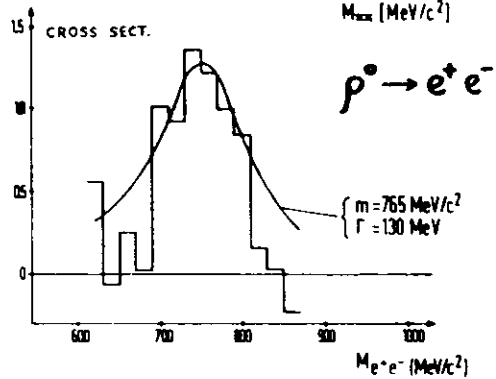
HARVARD (Wilson)

$\rho^\circ \rightarrow \mu^+ \mu^-$

$\Gamma_\rho = 97 \pm 20$ MeV

BR = (5.8 ± 1.2)

× 10^{-5}

EVTS/50 MeV

50

40

30

20

10

300   500   700   900   1100

DI-MUON MASS (MEV)
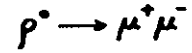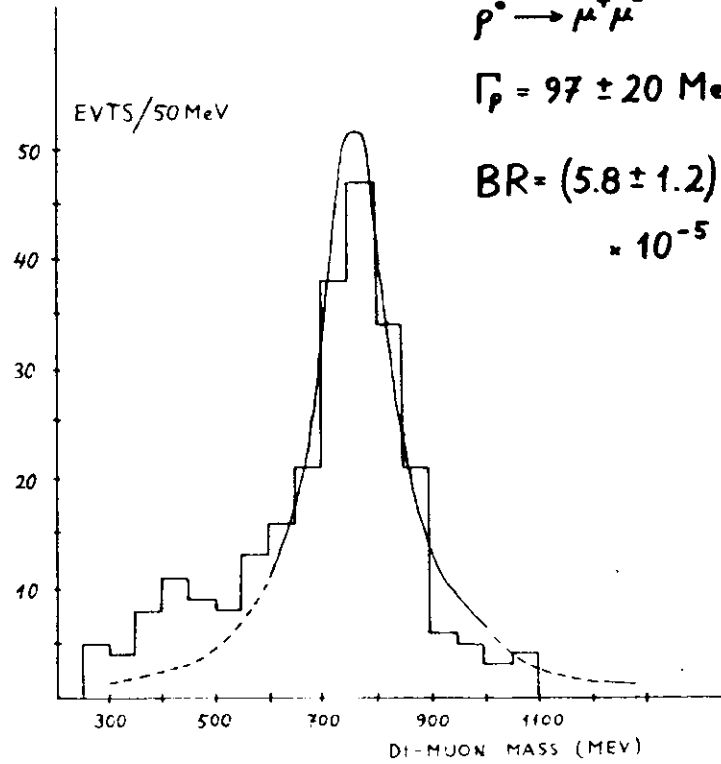
Fig. 5
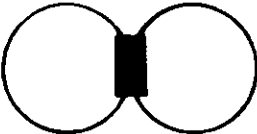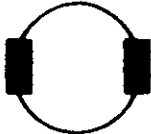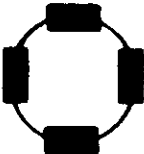
	Stanford	Novosibirsk	Orsay
Type of Machine	Weak Focusing	Weak Focusing	Strong Focusing
Number of Interacting Regions			
Bunch Length Length of Exp. Section	90 cm at 550 MeV 70 cm	90 cm at 385 MeV 70 cm	18 cm at 385 MeV 180 cm
Type of Collision	Angle Crossing	Head On	Head On
Currents $I_1 \times I_2$	70 mA $\times$ 70 mA (at 550 MeV)	20 mA $\times$ 50 mA (at 385 MeV)	5 mA $\times$ 5 mA (at 385 MeV)
Beam Lifetime	1/2 hour	1 hour	25 hours
Effective Luminosity	$5 \cdot 10^{31} cm^{-2} h^{-1}$	$3 \cdot 10^{30} cm^{-2} h^{-1}$	$5 \cdot 10^{30} cm^{-2} h^{-1}$
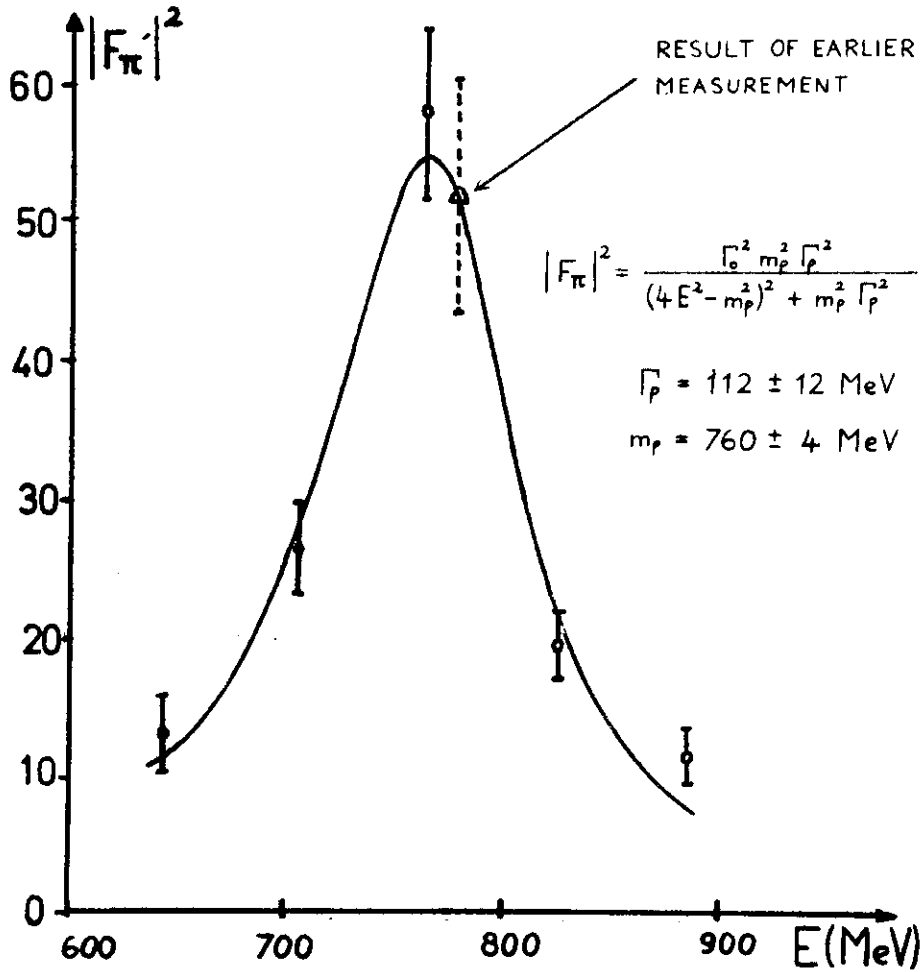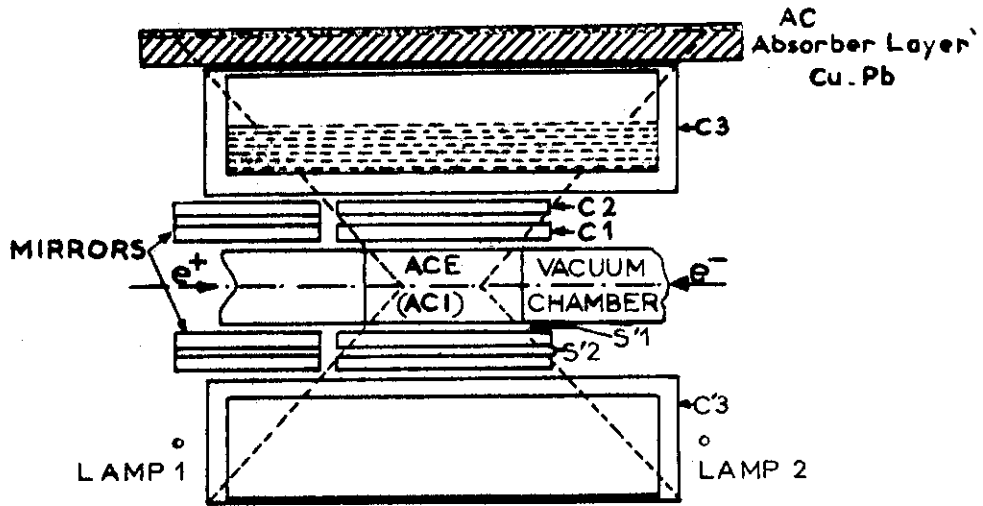
89649

Fig. 6

ORSAY - ρ - EXPERIMENT

Fig. 7

DESY — M.I.T.
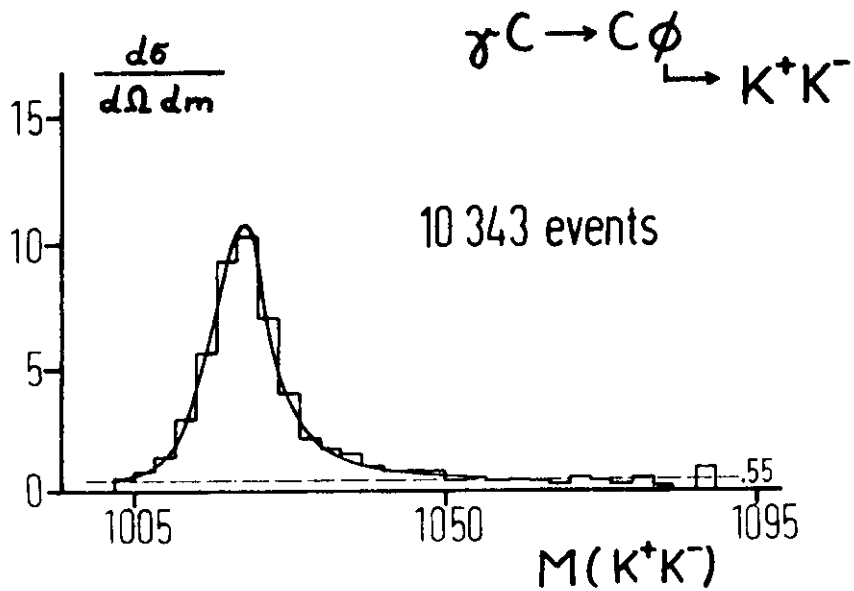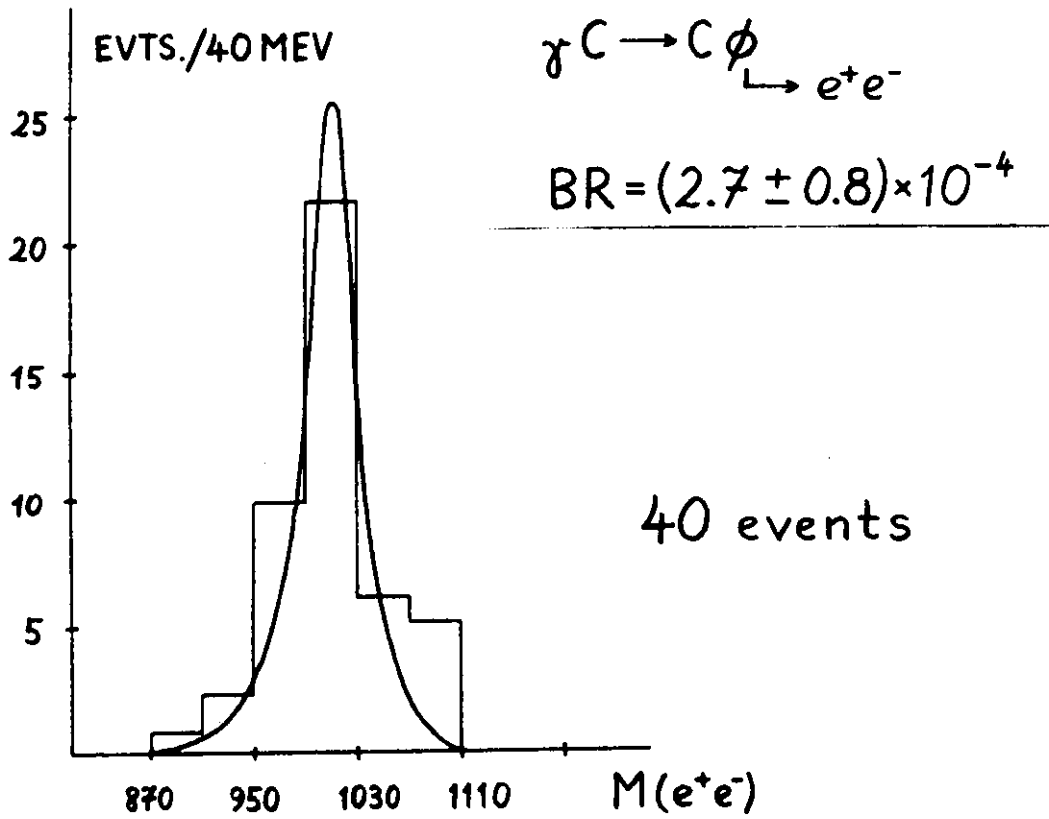
$\gamma C \longrightarrow C \phi$
$ \downarrow\!\!\! \longrightarrow e^+ e^-$

$$BR = (2.7 \pm 0.8) \times 10^{-4}$$

40 events

EVTS./40 MEV

M($e^+ e^-$)

$\gamma C \longrightarrow C \phi$
$ \downarrow\!\!\! \longrightarrow K^+ K^-$

10 343 events

$\frac{d\sigma}{d\Omega \, dm}$

M($K^+ K^-$)

Fig.8

Fig. 9

Fig. 10

DUBNA

$$\pi^- + p \longrightarrow V^\circ + n \longrightarrow e^+ e^-$$
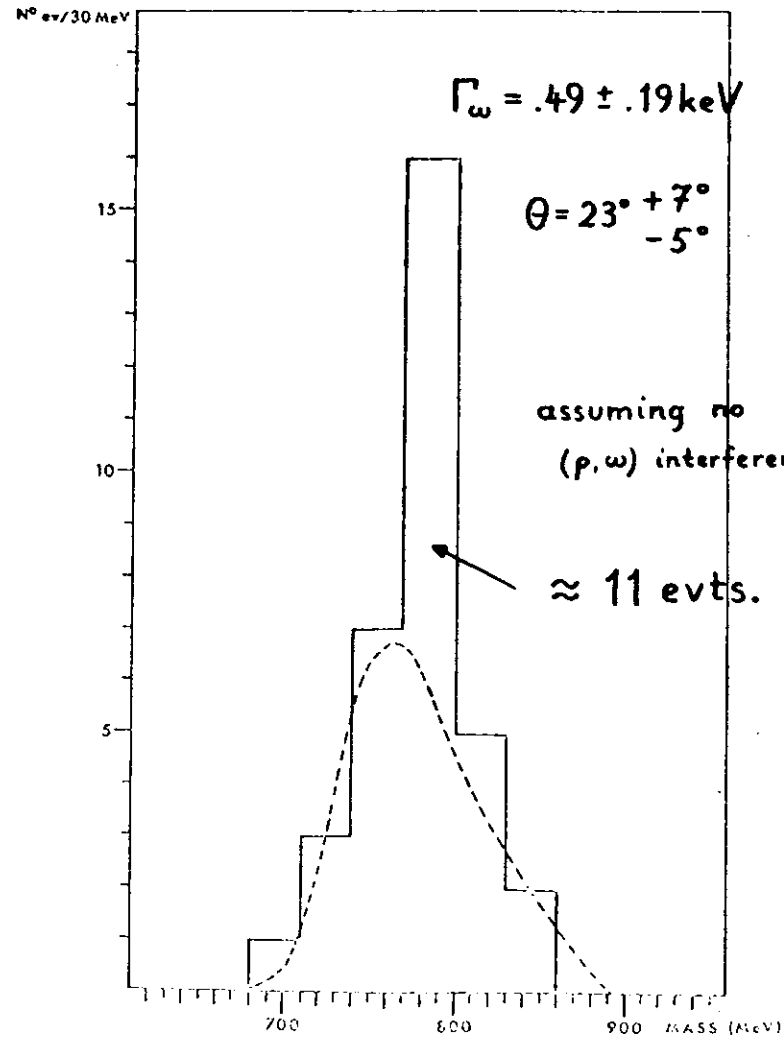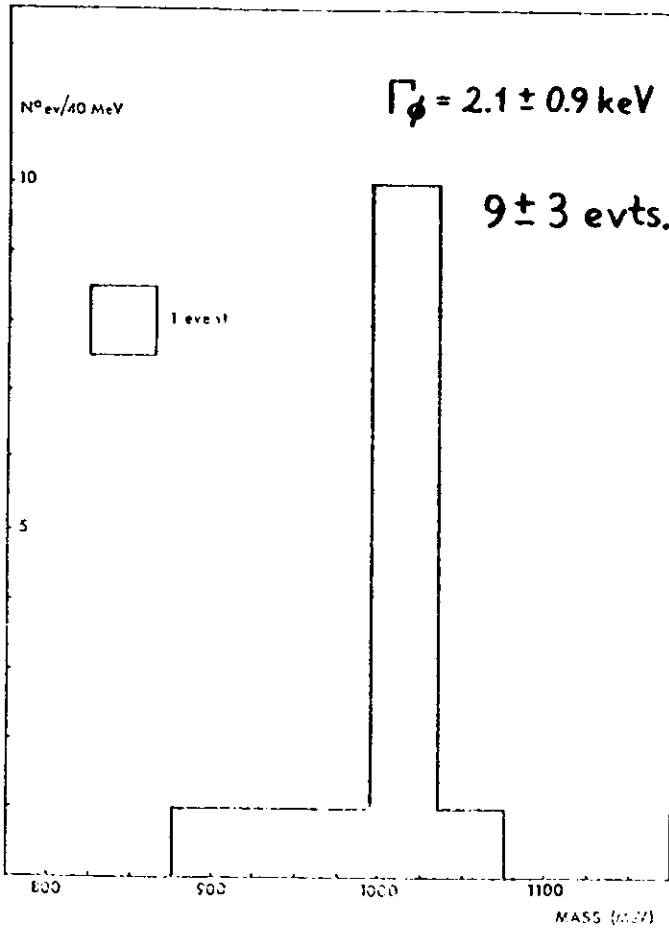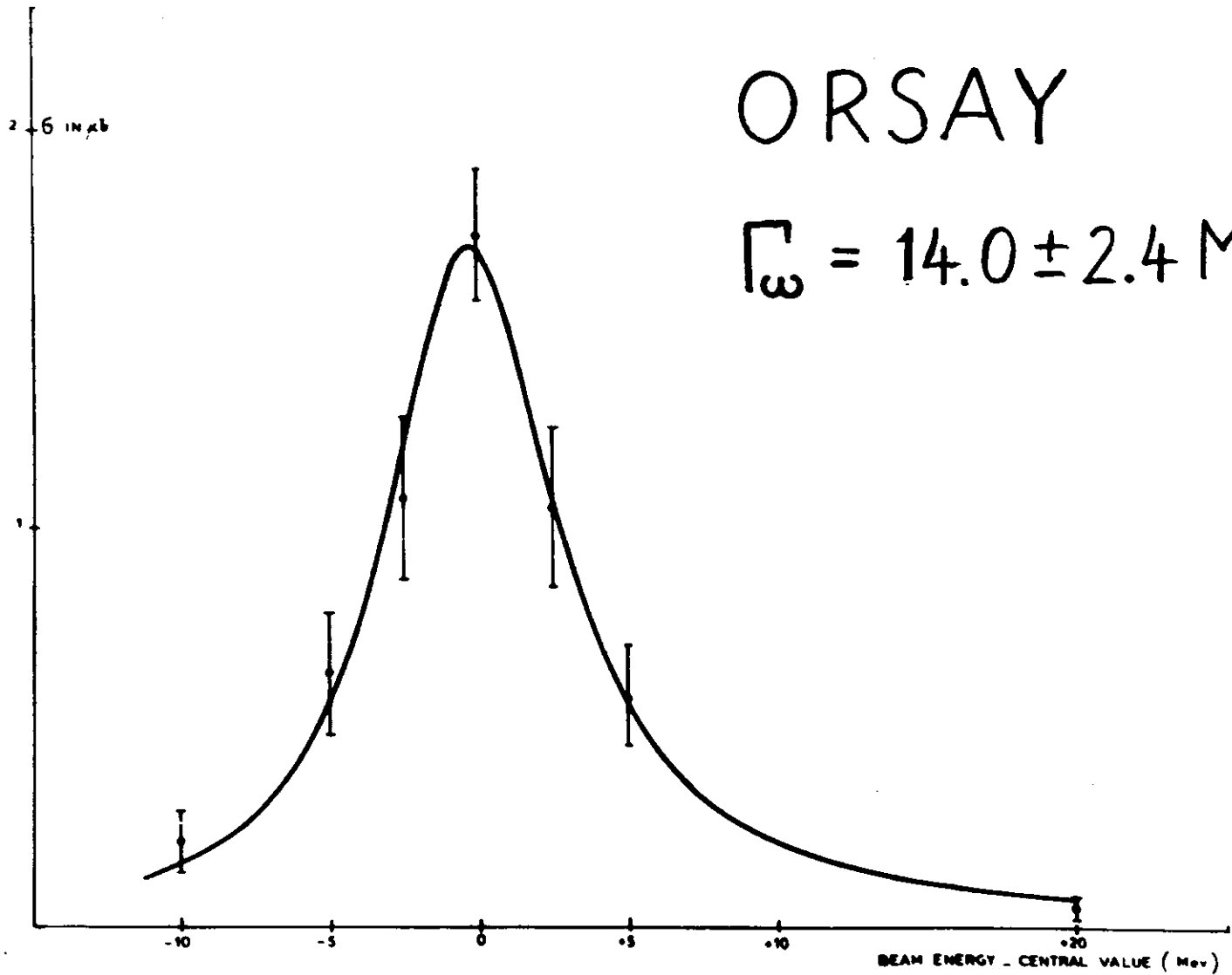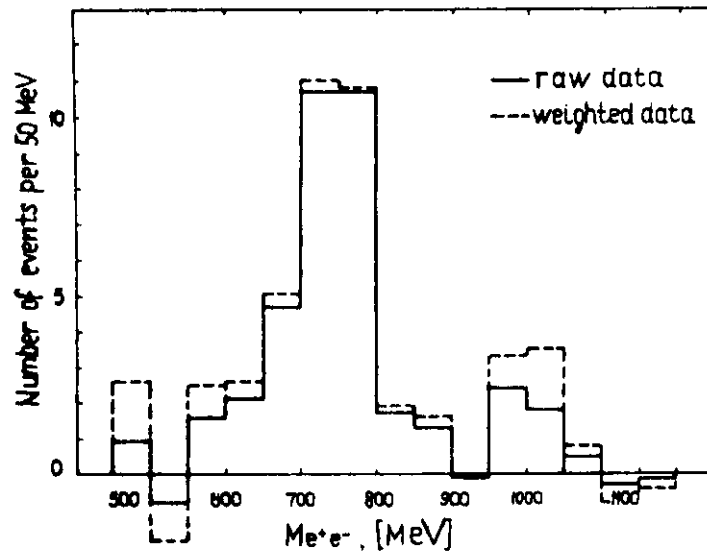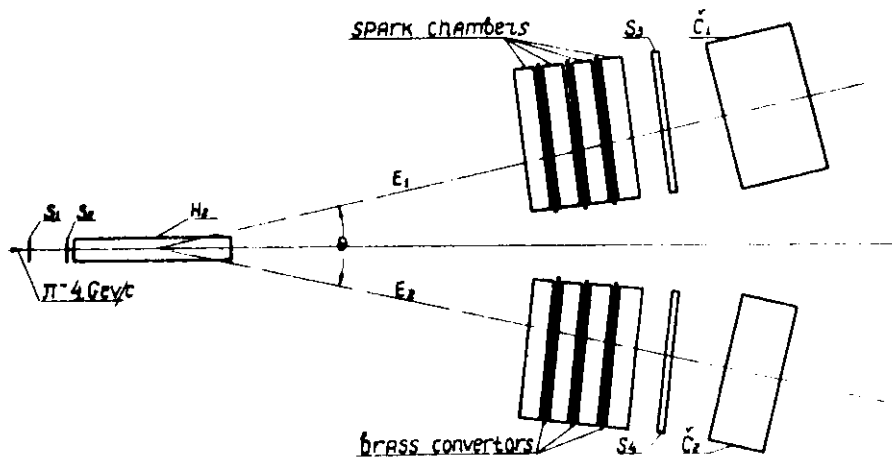
BASED ON SU(3): $B_\rho = (5.3 \pm 1.1) \times 10^{-5}$

$B_\omega = (6.5 \pm 1.3) \times 10^{-5}$ $B_\phi = (6.6 \begin{smallmatrix} +4.4 \\ -2.8 \end{smallmatrix}) \times 10^{-4}$

Fig.11

Comparison of the world average on leptonic decays of vector mesons with WEINBERG's 1st sum rule

$\sqrt{m_\omega \, \Gamma_{\omega \to ee}}$ (MeV)

$\sqrt{\dfrac{m_\rho \, \Gamma_{\rho \to ee}}{3}}$

$31.6 \pm \begin{smallmatrix} 3.9° \\ 4.9° \end{smallmatrix}$

$\sqrt{m_\phi \, \Gamma_{\phi \to ee}}$ (MeV)
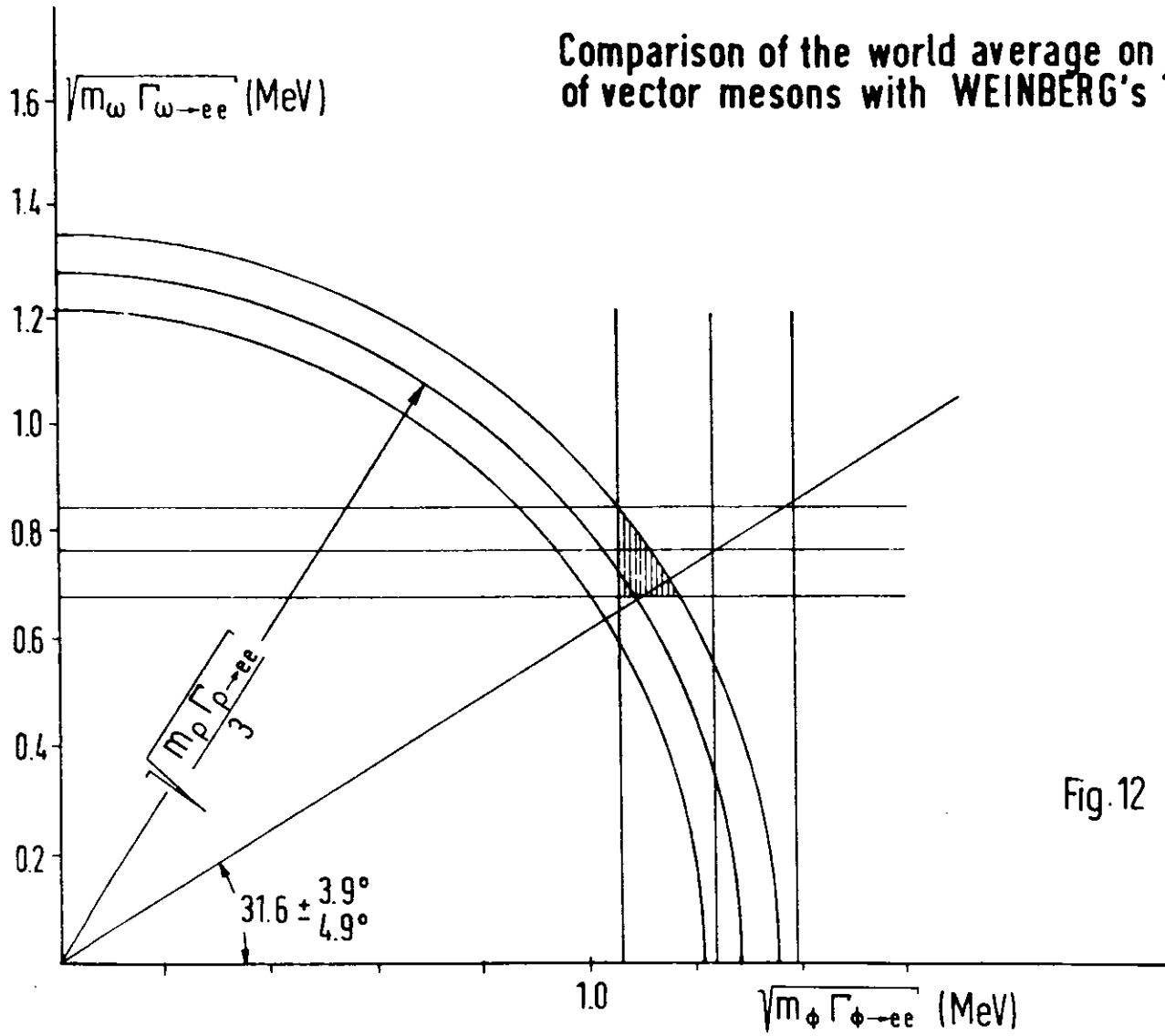
Fig. 12
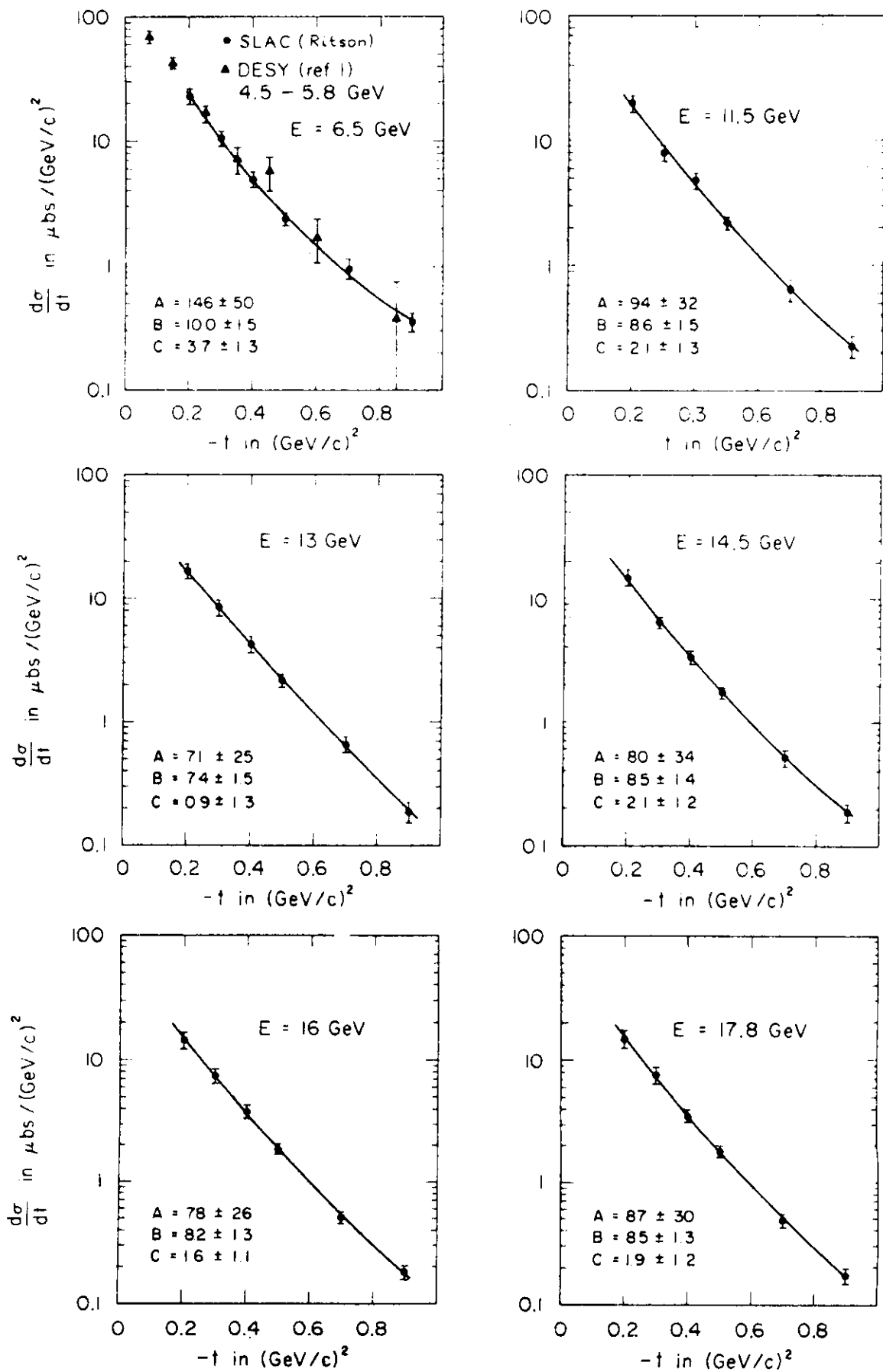
Fig.13
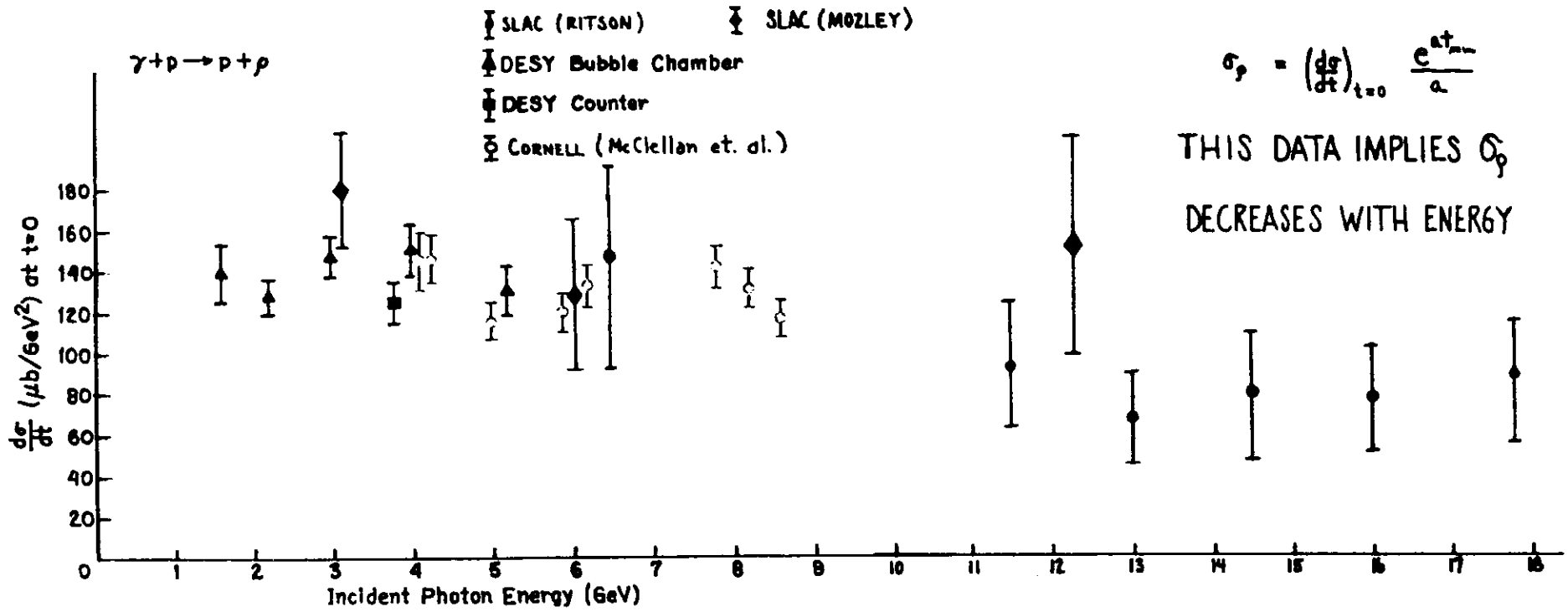
Fig.14

Fig.15

Fig.16

Fig.17

DESY $\dfrac{d\sigma\,(\gamma+d\rightarrow\rho^0+X)}{d\sigma\,(\gamma+p\rightarrow\rho^0+X)}$; $E_\gamma = 6$ GeV

CORNELL $\dfrac{d\sigma\,(\gamma+d\rightarrow\rho^0+d)}{d\sigma\,(\gamma+p\rightarrow\rho^0+p)}$; $2.1 < E_\gamma < 3.0$ GeV

$|t|$ (GeV^2)

DESY
CORNELL
$E_\gamma = 6$ GeV

$2.1 > E_\gamma > 3.0$ GeV

$3.0 > E_\gamma > 5.3$ GeV

Model of Trefil
$\sigma_{\rho N} = 30$ mb

$d\sigma/dt'$ (μb/GeV^2)

$|t'| = |t - t_{min}|$ (GeV^2)

$\dfrac{\frac{d\sigma}{d\Omega}\,(0^\circ, D_2)}{\frac{d\sigma}{d\Omega}\,(0^\circ, H_2)}$ $\dfrac{\gamma+d\rightarrow d'+p}{\gamma+p\rightarrow p+p}$ CORNELL

Average
= 2.87 ± .09

Incident Photon Energy (GeV)
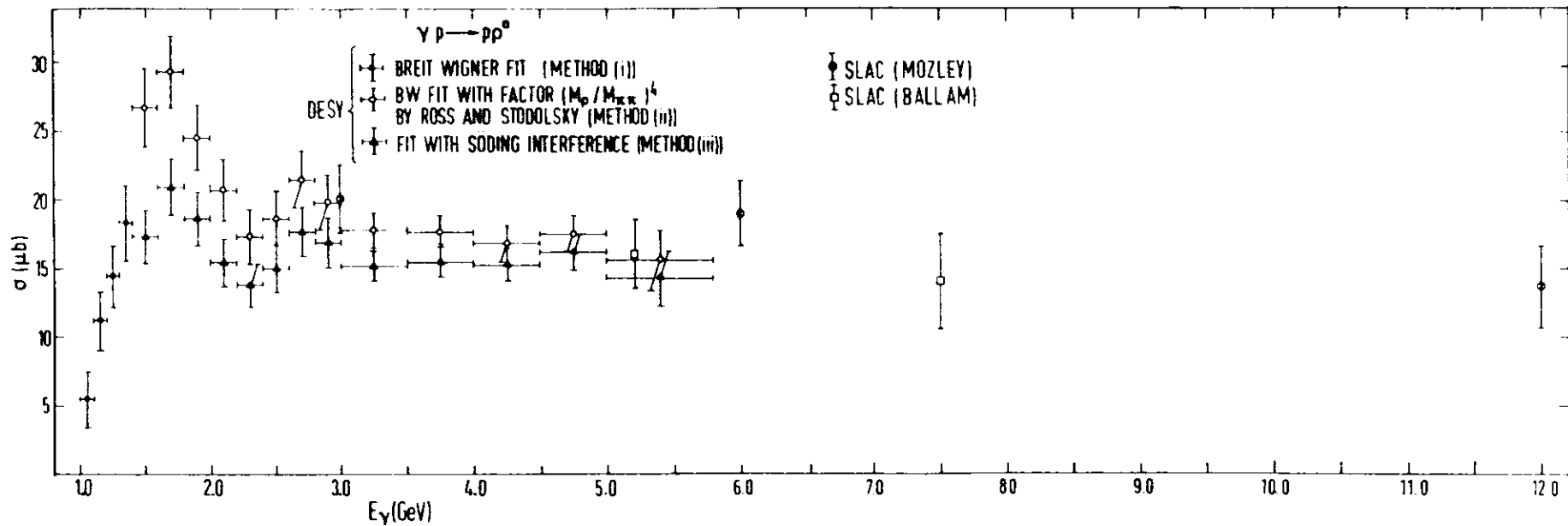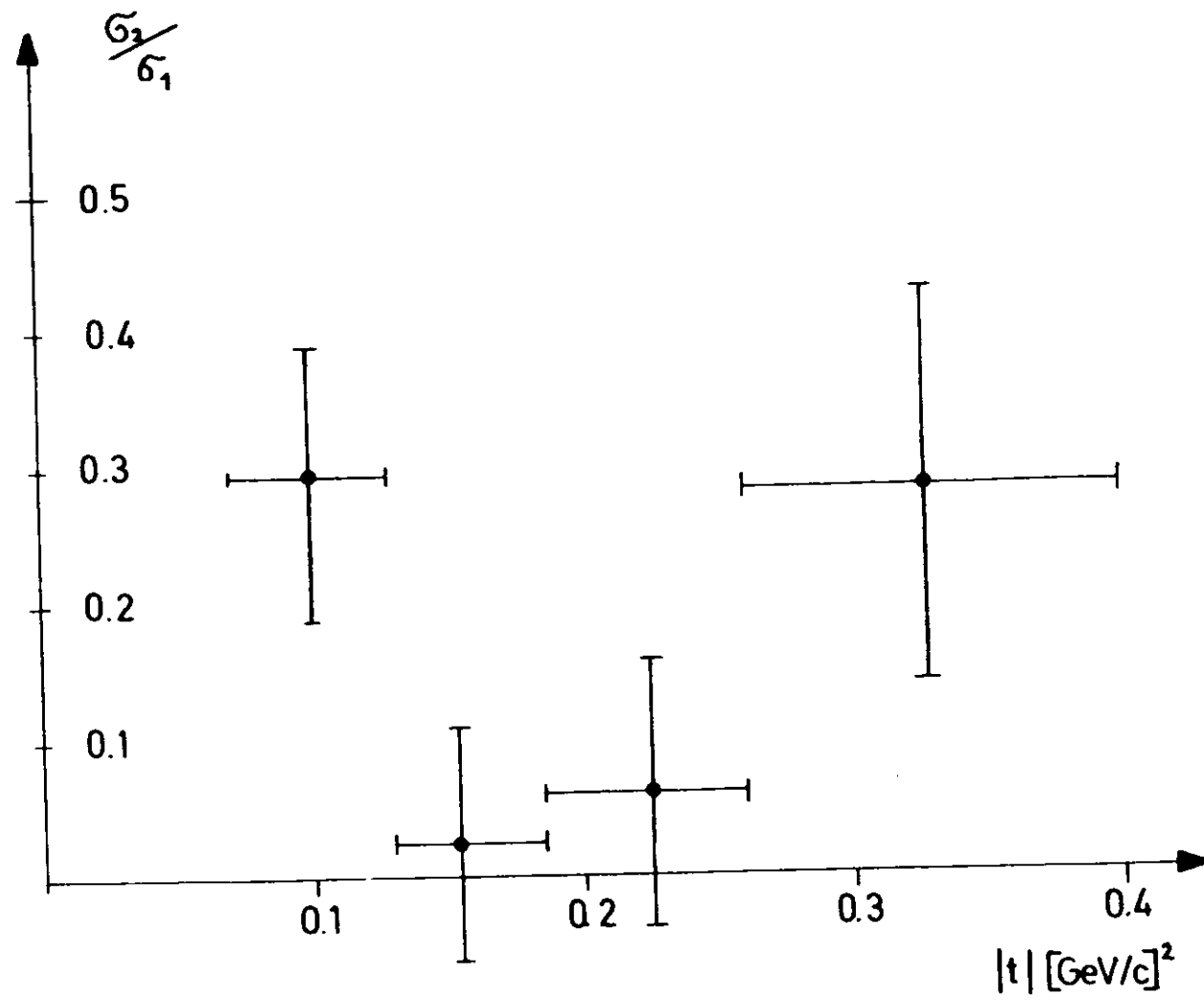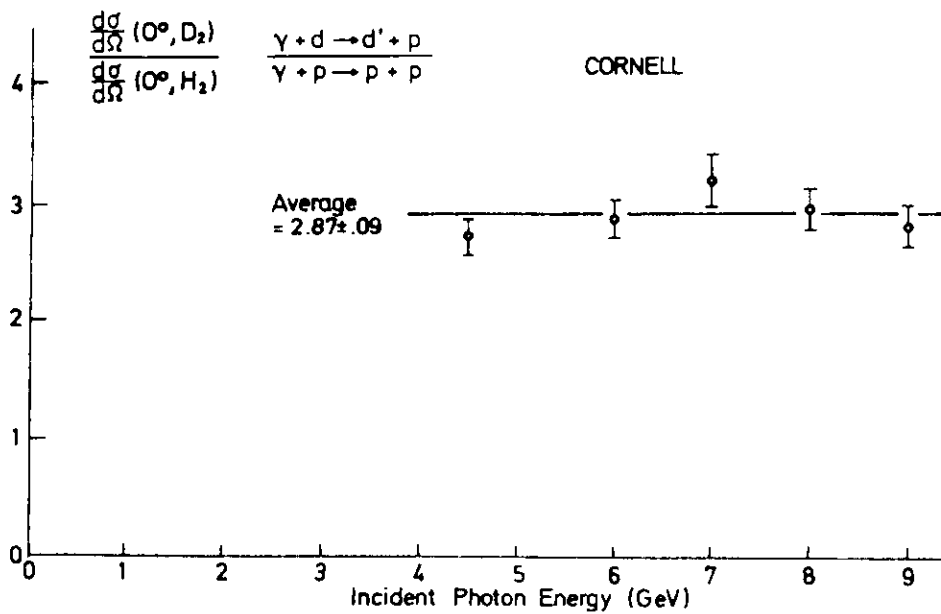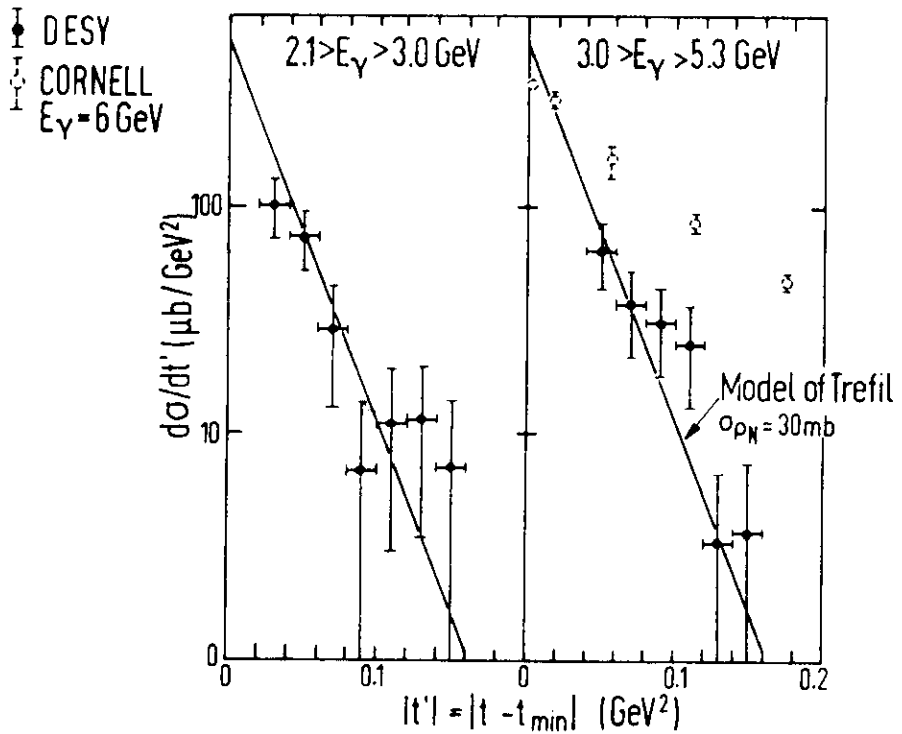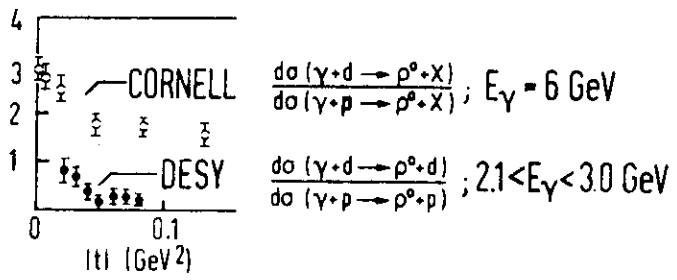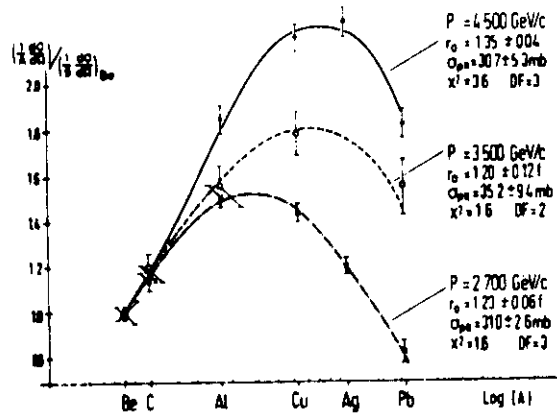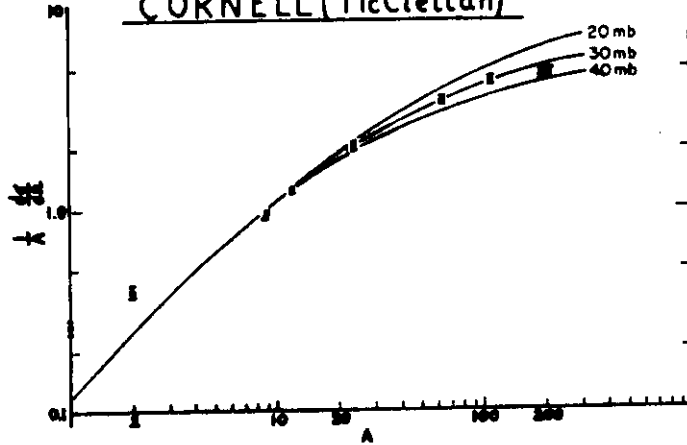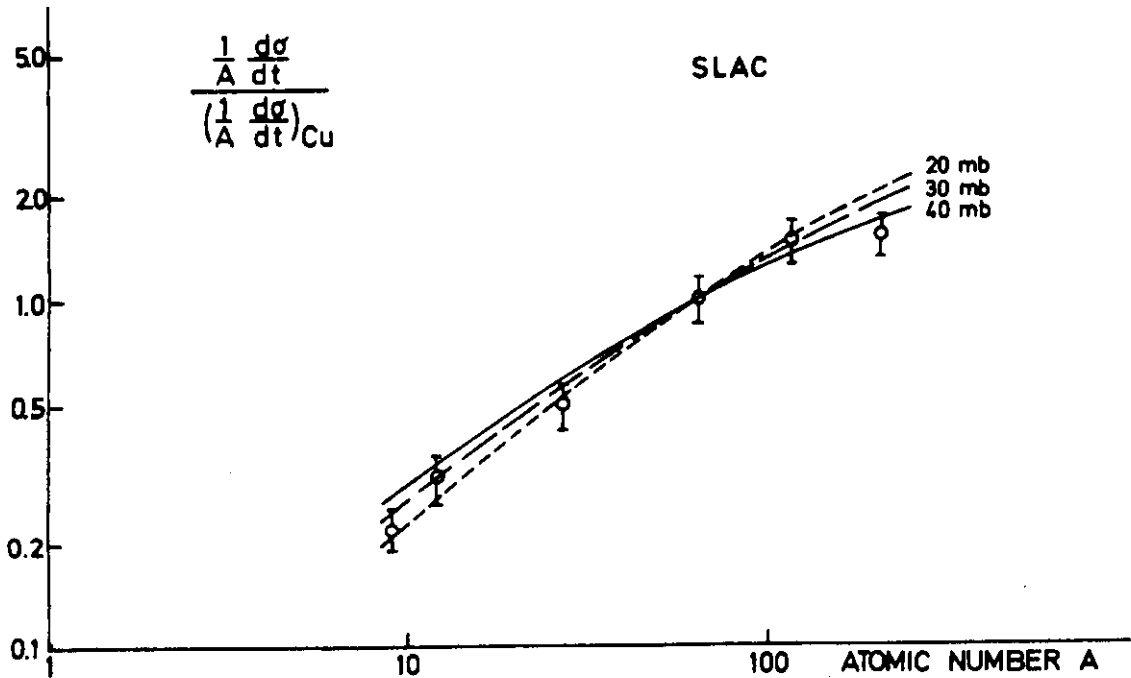
Fig.18

$$X(A) = \frac{\alpha}{4}\left(\frac{k}{4\pi}\right)^2 \frac{\sigma_T^2}{\frac{d\sigma}{d\Omega}(\gamma + A \to \rho + A)_{t=0}^{coh.}} \qquad \frac{\gamma\rho^2}{4\pi} = \lim_{A \to \infty} X(A)$$

DESY

CORNELL, $\sigma_T = \sigma_T(p+A)$ G.Belletini et al., Engler et.al.
CORNELL, $\sigma_T = \sigma_T(n+A)$ L.W.Jones et al., Pantuev et al.

$\rho \to e^+ e^-$, ρ MESON ON MASS SHELL
AND RESULTS FROM π FORM FACTOR,
$\sigma_T(\gamma p)$, $\gamma + p \to n + \pi^+$, $\gamma + n \to p + \pi^-$,
$\gamma + p \to p + \pi^0$, etc., WHERE THE
PHOTON IS ON THE MASS SHELL
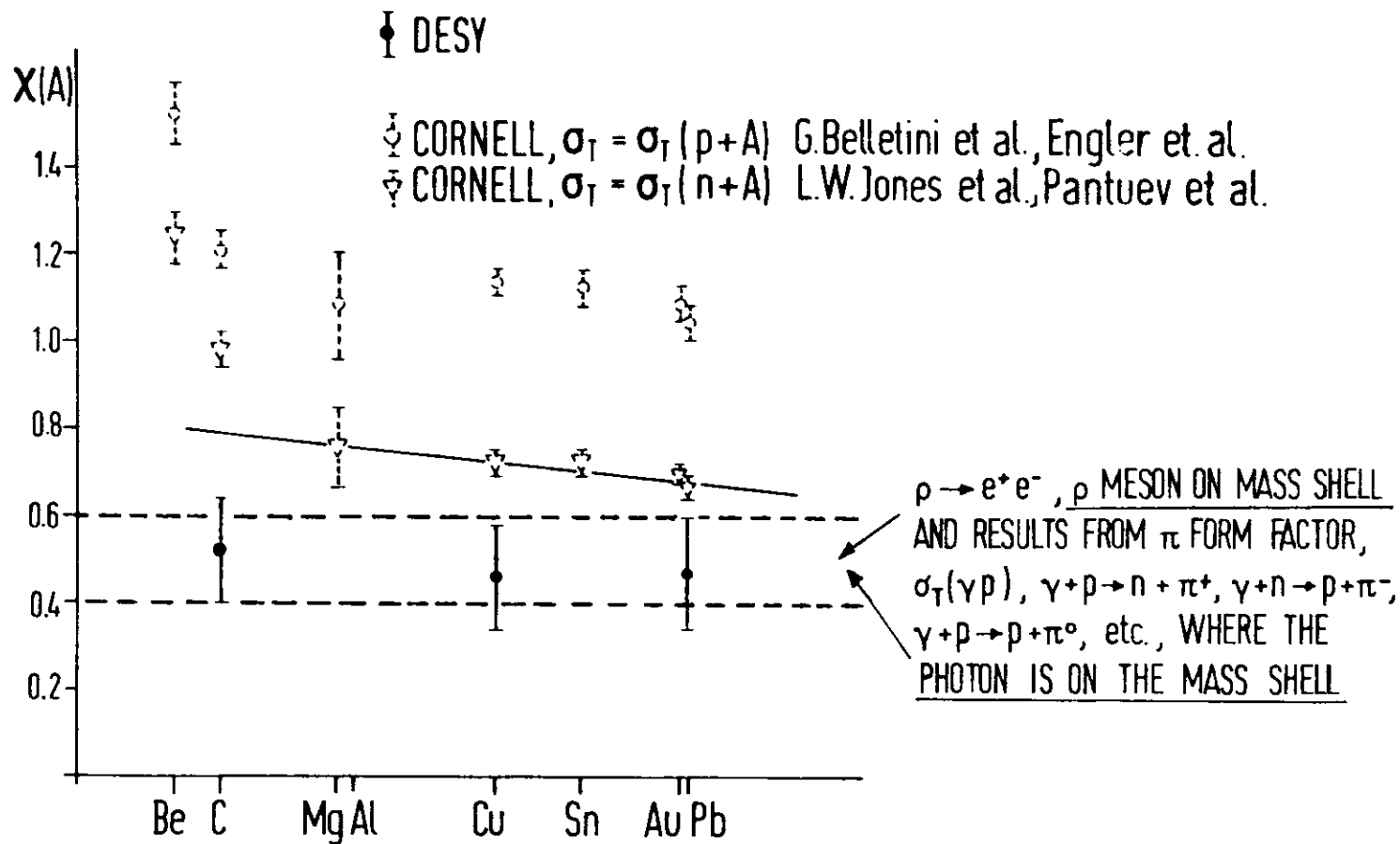
Fig.19

SLAC(Leith)
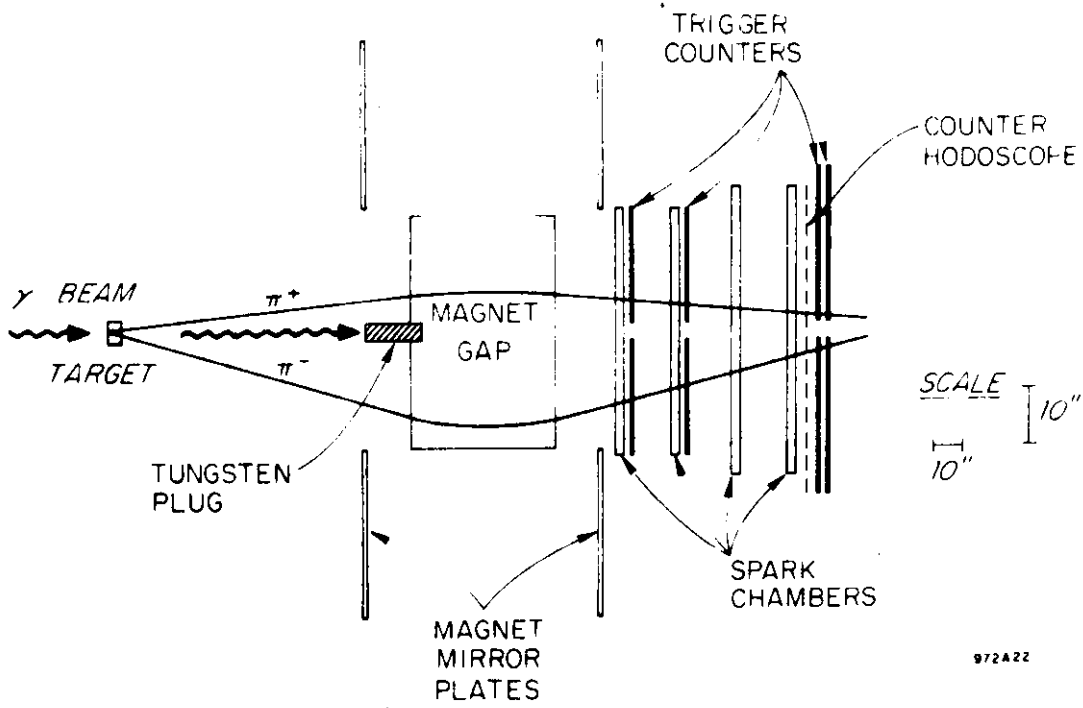
Fig. 20a

Fig. 20b

Fig. 21

Fig.22

$\gamma + p \longrightarrow p + \phi$
761 events

$\gamma + P \longrightarrow \phi + P$

SLAC
- o 13 GeV ϕ PRODUCTION
- ◘ 16 GeV ϕ PRODUCTION
- o 6 GeV (NEW DATA)
- △ 13 GeV (NEW DATA)

⊢●⊣ 2.5<E$_\gamma$<5.8 GeV DESY BUBBLE CHAMBER

▲ DESY-MIT COUNTER

Fig. 23

$\gamma + A \rightarrow A + \phi$ DESY—MIT

Be
991 events

C
10 343 events

Al
978 events

Cu
1 139 events

Ag
956 events

Pb
947 events

Fig. 24

$\gamma + A \rightarrow A + \phi$ *DESY-MIT*

Fig. 25

Fig. 26